expression of galactokinase was maintained by the mechanism of cells differentiating toward hepatocytes in HSM. The reason that galactokinase and GK were expressed in ES cells was not clear. One speculation is that these are crucial enzymes deeply involved in energy metabolism and important for the survival of ES cells.

Initially, HSM was expected to enrich hepatocytes differentiating from ES cells. Our data indicated that HSM promoted hepatocyte differentiation. Genes specific for hepatocytes are controlled by hepatocyte-specific transcription factors. To survive HSM, cells need to express hepatocyte-specific enzymes. Hepatocyte-specific transcription factors, therefore, are expressed, promoting hepatocyte differentiatin. This hypothesis is supported by the Northern blot analysis of C/EBPα and C/EBPβ, liver-specific transcription factors. These are more highly expressed in HSM than in ESM.

In the future, we will attempt to develop a method for harvesting large numbers of hepatocyte-like cells, focusing on extracellular matrix and growth factors. In the meanwhile, we recommend the development and refinement of the current method for human ES cells, with the eventual target of transplantation therapy for liver insufficiency.

**Acknowledgments** The authors thank Dr. Hitoshi Niwa (Center for Developmental Biology, Riken, Kobe, Japan) for providing EB5.

## References

Abe K, Niwa H, Iwase K, Takiguchi M, Mori M, Abe SI, Abe K, Yamamura KI (1996) Endoderm-specific gene expression in embryonic stem cells differentiated to embryoid bodies. Exp Cell Res 229:27–34

Ai Y, Jenkins NA, Copeland NG, Gilbert DH, Bergsma DJ, Stambolian D (1995) Mouse galactokinase: isolation, characterization, and location on chromosome 11. Genome Res 5:53–59

Barak V, Goike H, Panaretakis KW, Einarsson R (2004) Clinical utility of cytokeratins as tumor markers. Clin Biochem 37:529–540

Bossard P, Zaret KS (1998) GATA transcription factors as potentiators of gut endoderm differentiation. Development 125:4909–4917

Bradley MO (1977) Regulation of protein degradation in normal and transformed human cells. Effects of growth state, medium composition, and viral transformation. J Biol Chem 252:5310–5315

Gelly JL, Richoux JP, Grignon G, Bouhnik J, Baussant T, Alhenc-Gelas F, Corvol P (1991) Immunocytochemical localization of albumin, transferrin, angiotensinogen and kininogens during the initial stages of the rat liver differentiation. Histochemistry 96:7–12

Hamazaki T, Iiboshi Y, Oka M, Papst PJ, Meacham AM, Zon LI, Terada N (2001) Hepatic maturation in differentiating embryonic stem cells in vitro. FEBS Lett 497:15–19

Heo J, Factor VM, Uren T, Takahama Y, Lee JS, Major M, Feinstone SM, Thorgeirsson SS (2006) Hepatic precursors derived from murine embryonic stem cells contribute to regeneration of injured liver. Hepatology 44:1478–1486

Ichinose Y, Hashido K, Miyamoto H, Nagata T, Nozaki M, Morita T, Matsushiro A (1989) Molecular cloning and characterization of cDNA encoding mouse cytokeratin no. 19. Gene 80:315–323

Ikeda Y, Taniguchi N (2005) Gene expression of gamma-glutamyltranspeptidase. Methods Enzymol 401:408–425

Inoue C, Yamamoto H, Nakamura T, Ichihara A, Okamoto H (1989) Nicotinamide prolongs survival of primary cultured hepatocytes without involving loss of hepatocyte-specific functions. J Biol Chem 264:4747–4750

Ishizaka S, Shiroi A, Kanda S, Yoshikawa M, Tsujinoue H, Kuriyama S, Hasuma T, Nakatani K, Takahashi K (2002) Development of hepatocytes from ES cells after transfection with the HNF-3beta gene. FASEB J 16:1444–1446

Jones EA, Tosh D, Wilson DI, Lindsay S, Forrester LM (2002) Hepatic differentiation of murine embryonic stem cells. Exp Cell Res 272:15–22

Kumashiro Y, Asahina K, Ozeki R, Shimizu-Saito K, Tanaka Y, Kida Y, Inoue K, Kaneko M, Sato T, Teramoto K, Arii S, Teraoka H (2005) Enrichment of hepatocytes differentiated from mouse embryonic stem cells as a transplantable source. Transplantation 79:550–557

Lavon N, Benvenisty N (2005) Study of hepatocyte differentiation using embryonic stem cells. J Cell Biochem 96:1193–1202

Leffert HL, Paul D (1972) Studies on primary cultures of differentiated fetal liver cells. J Cell Biol 52:559–568

Longo L, Bygrave A, Grosveld FG, Pandolfi PP (1997) The chromosome make-up of mouse embryonic stem cells is predictive of somatic and germ cell chimaerism. Transgenic Res 6:321–328

Matsumoto K, Yamada K, Kohmura E, Kinoshita A, Hayakawa T (1994) Role of pyruvate in ischaemia-like conditions on cultured neurons. Neurol Res 16:460–464

McGee MM, Greengard O, Knox WE (1972) The quantitative determination of phenylalanine hydroxylase in rat tissues. Its developmental formation in liver. Biochem J 127:669–674

Miyashita H, Suzuki A, Fukao K, Nakauchi H, Taniguchi H (2002) Evidence for hepatocyte differentiation from embryonic stem cells in vitro. Cell Transplant 11:429–434

Murakami T, Nishiyori A, Takiguchi M, Mori M (1990) Promoter and 11-kilobase upstream enhancer elements responsible for hepatoma cell-specific expression of the rat ornithine transcarbamylase gene. Mol Cell Biol 10:1180–1191

Nagy P, Bisgaard HC, Thorgeirsson SS (1994) Expression of hepatic transcription factors during liver development and oval cell differentiation. J Cell Biol 126:223–233

Nakamura T, Teramoto H, Tomita Y, Ichihara A (1984) L-proline is an essential amino acid for hepatocyte growth in culture. Biochem Biophys Res Commun 122:884–891

Niwa A, Yamamoto K, Sorimachi K, Yasumura Y (1980) Continuous culture of Reuber hepatoma cells in serum-free arginine-, glutamine- and tyrosine-deprived chemically defined medium. In Vitro 16:987–993

Niwa H, Masui S, Chambers I, Smith AG, Miyazaki J (2002) Phenotypic complementation establishes requirements for specific POU domain and generic transactivation function of Oct-3/4 in embryonic stem cells. Mol Cell Biol 22:1526–1536

Ohira RH, Dipple KM, Zhang YH, McCabe ER (2005) Human and murine glycerol kinase: influence of exon 18 alternative splicing on function. Biochem Biophys Res Commun 331:239–246

Phillips JW, Jones ME, Berry MN (2002) Implications of the simultaneous occurrence of hepatic glycolysis from glucose and gluconeogenesis from glycerol. Eur J Biochem 269: 792–797

Shiojiri N (1997) Development and differentiation of bile ducts in the mammalian liver. Microsc Res Tech 39:328–335

Shiojiri N, Lemire JM, Fausto N (1991) Cell lineages and oval cell progenitors in rat liver development. Cancer Res 51:2611–2620

Shiojiri N, Takeshita K, Yamasaki H, Iwata T (2004) Suppression of C/EBP alpha expression in biliary cell differentiation from

hepatoblasts during mouse liver development. J Hepatol 41:790–798

Soto-Gutierrez A, Kobayashi N, Rivas-Carrillo JD, Navarro-Alvarez N, Zhao D, Okitsu T, Noguchi H, Basma H, Tabata Y, Chen Y, Tanaka K, Narushima M, Miki A, Ueda T, Jun HS, Yoon JW, Lebkowski J, Tanaka N, Fox IJ (2006) Reversal of mouse hepatic failure using an implanted liver-assist device containing ES cell-derived hepatocytes. Nat Biotechnol 24:1412–1419

Sumida KD, Crandall SC, Chadha PL, Qureshi T (2002) Hepatic gluconeogenic capacity from various precursors in young versus old rats. Metabolism 51:876–880

Teramoto K, Hara Y, Kumashiro Y, Chinzei R, Tanaka Y, Shimizu-Saito K, Asahina K, Teraoka H, Arii S (2005) Teratoma formation and hepatocyte differentiation in mouse liver transplanted with mouse embryonic stem cell-derived embryoid bodies. Transplant Proc 37:285–286

Teratani T, Yamamoto H, Aoyagi K, Sasaki H, Asari A, Quinn G, Sasaki H, Terada M, Ochiya T (2005) Direct hepatic fate specification from mouse embryonic stem cells. Hepatology 41:836–846

Wheatley DN, Scott L, Lamb J, Smith S (2000) Single amino acid (arginine) restriction: growth and death of cultured HeLa and human diploid fibroblasts. Cell Physiol Biochem 10:37–55

Yamada T, Yoshikawa M, Kanda S, Kato Y, Nakajima Y, Ishizaka S, Tsunoda Y (2002) In vitro differentiation of embryonic stem cells into hepatocyte-like cells identified by cellular uptake of indocyanine green. Stem Cells 20:146–154

Yoshida-Koide U, Matsuda T, Saikawa K, Nakanuma Y, Yokota T, Asashima M, Koide H (2004) Involvement of Ras in extraembryonic endoderm differentiation of embryonic stem cells. Biochem Biophys Res Commun 313:475–481

Zaret KS (2002) Regulatory phases of early liver development: paradigms of organogenesis. Nat Rev Genet 3:499–512

Original Paper

# Contrast-enhanced US with Levovist for the Diagnosis of Hepatic Hemangioma: Time-related Changes of Enhancement Appearance and the Hemodynamic Background

*Satoshi Kobayashi[1], Hitoshi Maruyama[1], Hidehiro Okugawa[1], Hiroaki Yoshizumi[1]*
*Shoichi Matsutani[2], Masaaki Ebara[1], Osamu Yokosuka[1]*
[1]Department of Medicine and Clinical Oncology, Chiba University Graduate School of Medicine and [2]Chiba College of Health Science, Chiba, Japan
Corresponding Author: Hitoshi Maruyama, Department of Medicine and Clinical Oncology
Chiba University Graduate School of Medicine, 1-8-1 Inohana, Chuou-ku, Chiba 260-8670, Japan
Tel: +81 43 226 2083, Fax: +81 43 226 2088, E-mail: maru@faculty.chiba-u.jp

**KEYWORDS:**
Liver; Hemangioma; Ultrasound; Contrast agent

**ABBREVIATIONS:**
Magnetic Resonance Imaging (MRI); Contrast-Enhanced Computed Tomography (CECT); Ultrasound (US); Contrast-Enhanced US (CEUS); Hepatocellular Carcinoma (HCC); Mechanical Index (MI); Arterioportal Shunt (AP shunt); Microbubble Disappearance Time (MD-T); Nodular Enhancement (NE)

## ABSTRACT

**Backgrounds/Aims:** To elucidate the diagnostic confidence of contrast-enhanced ultrasound (CEUS) with Levovist for hepatic hemangioma.

**Methodology:** The subjects were 34 patients with 38 hemangiomas and 12 patients with 15 hypervascular hepatocellular carcinomas. The early-phase (15-60 second) and liver-specific phase (after 5 min) were observed by the first injection. The 2nd injection was done for solo-phase method to observe liver-specific phase images without taking early-phase sonograms. The 3rd injection was done for changing posture method to observe liver-specific sonograms under left lateral ducubitus position.

**Results:** In the early-phase of hemangioma, nodular enhancement (NE) was found transiently in 13 lesions (34%) and continuously in 25 lesions (66%), while hepatocellular carcinoma (HCC, n=15) did not show this pattern. Intratumoral arterioportal shunt was closely related to the short duration of NE. Two enhancement patterns were observed in the liver-specific phase of hemangioma, diffuse in 12 lesions (31%) and partial in 26 lesions (69%), which were dependent on the early-phase enhancement. Liver-specific findings were also affected by taking early-phase sonograms or changing the posture of the patient. This method provided sensitivity of 79% and specificity of 100% for the diagnosis of hemangioma.

**Conclusions:** CEUS with Levovist may be promising method for the diagnosis of hepatic hemangioma.

## INTRODUCTION

Recent advances in digital technologies have resulted in remarkable developments in the field of imaging diagnosis for focal liver lesions (1-4). Although percutaneous needle biopsy has been an essential procedure for the diagnostic standard of liver tumors, there are expectations for their characterization by imaging modalities as a non-invasive method (5-7).

Cavernous hemangioma is the most common tumor among benign focal lesions in the liver (8). Magnetic resonance imaging (MRI) or contrast-enhanced computed tomography (CECT) usually makes the diagnosis, because they have high diagnostic ability based on the characteristic pattern of the tumor (9,10). However, high reliability by ultrasound (US) examination for the diagnosis of hemangioma would be preferable, in terms of the advantages of real-time observation, simple technique and non-invasiveness in clinical practice.

With the development of microbubble contrast agents, contrast-enhanced US (CEUS) has frequently been used for the characterization of liver tumors (1,2,11-15). As for the diagnosis of hemangioma, nodular enhancement (NE) is known as a characteristic enhancement pattern (16-18), and positive enhancement in liver-specific phase is considered to be a characteristic finding of benign liver lesions (14,15). However, some different enhancement patterns have also been reported in CEUS findings of hemangioma (16-18). The variety of the enhancement patterns might be caused by changes of NE during the course of the early-phase enhancement. In addition, static but unstable status of microbubble were supposed to be the causes of different liver-specific patterns, because hemangioma has quite slow blood flow and lacks Kupffer cells which may cause concern about microbubble accumulation in the liver (16-19).

According to this background, CEUS were examined with Levovist both in hepatic hemangioma and HCC, and the time-related changes of contrast-

Hepato-Gastroenterology 2008; 55:1222-1228

enhanced appearances in these 2 tumors were carefully analyzed to present the features of enhancement patterns of hemangioma. Moreover, whether the early-phase observation prior to liver-specific phase or posture of the patient may affect the liver-specific images of hemangioma and HCC was examined to prove the various pattern of liver-specific images of hemangioma. The aim of this study was to elucidate the diagnostic confidence of CEUS with Levovist for hemangioma.

## METHODOLOGY

### Patients

From July 2005 to January 2007, 34 patients with 38 cavernous hemangiomas in the liver were enrolled in this retrospective study. They consisted of 12 men and 22 women aged from 29-86 years (58±12, mean ± SD). The diagnosis of hemangioma was obtained by CECT in 14 lesions and MRI in 24 lesions, and the size of the lesions ranged from 9.5-137mm (27±22). The number of lesions was one in 31 patients, 2 in 2 patients and 3 in 1 patient and their US pattern were hyperechoic in 22 lesions and hypoechoic in 16 lesions. Thirty patients had normal liver, 3 patients had fatty liver, and 1 patient had liver cirrhosis related to hepatitis C virus.

During the same period, 56 patients with 59 hypervascular HCC lesions underwent CEUS examination before treatment. Among them, additional CEUS examinations to compare their contrast-enhanced findings with hemangioma were done in 12 patients who had enough time for the observation of contrast enhancement under the extra injection of contrast agent. They consisted of 9 men and 3 women aged from 67-83 years (27±10), and all had liver cirrhosis with 15 HCC lesions. Ten patients had hepatitis C virus, but the other 2 patients had neither hepatitis B nor hepatitis C virus. The size of the lesions ranged from 15-52mm (27±10). The diagnosis of HCC was obtained by CECT in 10 lesions and percutaneous needle biopsy in 5 lesions. The depth of the lesions measured between skin surface and its nearest edge of the lesion was 20-100mm (47±22) for hemangioma and 40-100mm (65±25) for HCC.

Therefore, the subjects of this retrospective study were 34 patients with 38 hemangioma and 12 patients with 15 HCCs. Informed consent was obtained by all patients and institutional ethics committee approval was not deemed to be necessary by the chair person for the present study.

### Imaging Methods for the Diagnosis of Hemangioma

CECT was performed using Light speed ultra 16 (GE Yokogawa Medical Systems, Hino, Japan). After the injection of 100mL of contrast medium (Iopamiron 300; Nihon Schering, Osaka, Japan) into the antecubital vein at a rate of 3.0mL/s, three-phase images were taken with 5mm collimation (30-s-delay for arterial phase, 80-s-delay for portal phase, and 180-s-delay for equilibrium phase). Imaging criteria for CT images for the diagnosis of hemangioma was a globular peripheral enhancement followed by centripetal fill-in in the arterial phase or a homogenous enhancement in the arterial phase and persistent enhancement during portal phase and were isoattenuating with enhanced intrahepatic vessels (9,20).

MRI was performed using a superconducting system (Signa Horizen; GE Yokogawa Medical Systems, Hino, Japan) operating at 1.5 T. Axial spin-echo (SE) pulse sequences were employed with a repetition time ($T_R$) of 500ms and an echo time ($T_E$) of 11ms for $T_{1W}$ and $T_R$ of 2000ms and $T_E$ of 80ms for $T_{2W}$. T1FS were obtained at $T_R$ of 500ms and $T_E$ of 11ms using the chemical shift selective technique to suppress the fat signal. Imaging criteria by MRI for the diagnosis of hemangioma were both low signal intensity on $T_1$-weighted images and high signal intensity on $T_2$-weighted images, and high signal intensity on proton-weighted images (10). All the images of CT and MRI were reviewed by M.E., a hepatologist specialized in the reading of CT and MRI images.

### US Examination

US examinations were performed with SSA-770A (APLIO, Toshiba, Tokyo, Japan) with a 3.75MHz convex probe. Non-contrast US was performed by tissue harmonic imaging (THI 2.5/5.0), and CEUS was done by wide-band Doppler mode (Advanced Dynamic Flow mode) with intermittent scanning (approximately 1-s intervals). Monitor imaging mode under extra-low mechanical index (MI<0.2) was used to keep the scan plane to support the interval observation. The MI values were between 1.0 and 1.4, and the focal position was set at the bottom of the lesion. The US contrast agent was Levovist (Schering AG, Berlin, Germany), consisting of galactose microparticles (99.9%) and palmitic acid (0.1%). It was administered at a dose of 5.0mL at 300mg/mL (standard dose in Japan) from the antecubital vein as a bolus at a rate of 2.0mL/s followed by a 5mL normal saline flush. After observation with non-contrast US, color Doppler imaging for the lesion was performed to investigate the intratumoral blood flow. When two-parallel vessels showing increased arterial blood flow with reversed blood flow were observed in the lesion on the sonogram, the lesion was diagnosed as hemangioma with intratumoral arterioportal shunt (AP shunt) (21,22). Contrast-enhanced images were taken almost at the median section under breath-holding.

All patient, 34 patients with 38 hemangioma and 12 patients with 15 HCC, received injections of Levovist 3 times, and each injection was done after the disappearance of the prior enhancement. In the present study, the early-phase was defined as the phase 15-60 seconds after the injection and liver-specific phase was defined as the phase contrast enhancement in the portal vein disappeared by the observation of MD-T (23).

US examination was performed by S.K. in 38 patients and by H.Y. in 8 patients, and all sonograms

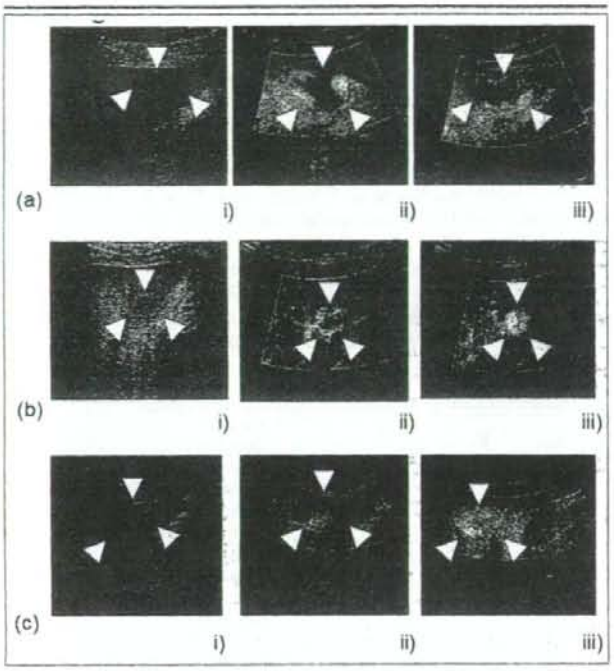


**FIGURE 1** Time-related changes of contrast enhancement of hemangioma at the early-phase **(a)** Continuous type. i) Gray-scale. Hyperechoic lesion was seen at segment III in the liver (39mm, arrowheads). ii) Contrast-enhanced sonogram of early-phase (40 s after injection). NE was observed in the lesion. iii) Contrast-enhanced sonogram of early-phase (50 s after injection). NE was observed in the lesion. **(b)** Transient type A. i) Grayscale. Hypoechoic lesion was seen at the segment V in the liver (19mm, arrowheads). ii) Contrast-enhanced sonogram of early-phase (31 s after injection). NE was observed in the lesion. iii) Contrast-enhanced sonogram of early-phase (37 s after injection) The lesion showed whole enhancement following NE, earlier than enhancement of surrounding liver parenchyma. (c) Transient type B. i) Grayscale. Hypoechoic lesion was seen at the segment III in the liver (40mm, arrowheads). ii) Contrast-enhanced sonogram of early-phase (30 s after injection). NE was observed in the lesion. iii) Contrast-enhanced sonogram of early-phase (48 s after injection). The lesion showed whole enhancement following NE, similar to the progression of enhancement in surrounding liver parenchyma.

digitally stored were reviewed by the consensus of H.M. and H.O. The observers and reviewers were hepatologists specialized in US examination.

### Standard Method by First Injection

Observation of the early-phase, and subsequent liver-specific phase following the stopping of US transmission to avoid the microbubble breakdown was done under the supine position.

### Solo-phase Method by Second Injection

Liver-specific phase images were taken at the time of MD-T without scanning the prior early-phase under the supine position. Contrast-enhanced areas in lesions on liver-specific sonograms were compared quantitatively between the images after taking prior early-phase sonograms and those without taking them, by measurement of the pixel count using Scion Image (Scion Corp., Frederick, MD, USA).

### Changing Posture Method by Third Injection

After the observation of the early-phase with the supine position, scanning was stopped and the posture of the patient was changed to the left lateral decubitus position. The same posture was kept until MD-T, and liver-specific sonograms were taken. Liver-specific images by the first injection were compared quantitatively with the images obtained by the changing posture method. The lesion on the sonogram was divided into tetrameric portions by horizontal line and vertical line, and the change of the portions with maximum enhancement between the 2 liver-specific images by 2 methods was considered to be a positive result for the changing posture method.

### Statistical Analysis

The Tukey-Kramer test was used to compare the times to continue NE among 3 groups. The chi-square test was used to analyze the relationship between hemangioma and HCC in the solo-phase method and the changing posture method. Stat View version 5 (Abacus Concepts Inc., Berkeley, CA) was employed for the above statistical analysis. The difference with a probability of <5% was considered to be statistically significant ($p<0.05$).

## RESULTS

### Contrast Enhancement at the Early Phase of Hemangioma

Early-phase sonograms are shown in **Figure 1**. NE was found in all lesions, with 13 lesions showing transiently in the earliest part of the early-phase (transient type, 34%) and 25 lesions showing contin-

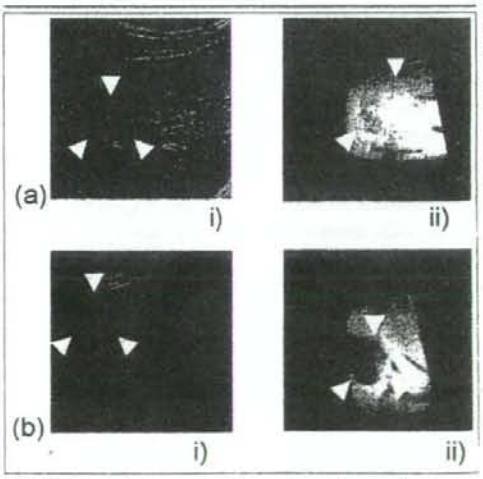


**FIGURE 2** Contrast enhancement of hemangioma at liver-specific phase **(a)** Type 1 (diffuse enhancement). i) Grayscale. Hyperechoic lesion was seen at segment VIII in the liver (18mm, arrowheads). ii) Contrast-enhanced sonogram of liver-specific phase. The lesion had diffuse enhancement appearance. (b) Type 2 (partial enhancement). i) Grayscale. Hyperechoic lesion was seen at segment VIII in the liver (36mm, arrowheads). ii) Contrast-enhanced sonogram of liver-specific phase. The lesion had partial enhancement appearance.

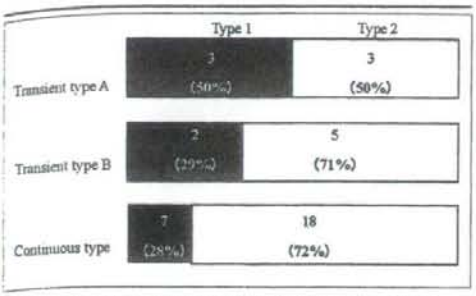


**FIGURE 3** Relationship of contrast-enhanced patterns of hemangioma between early-phase and liver-specific phase. Contrast-enhanced findings of liver-specific phase depended on the extent and rapidity of early-phase enhancement in the lesion. Transient type A, B, Continuous type: Early phase. Transient type A: NE was observed transiently in earliest part of early-phase, followed by the whole enhancement of the lesion earlier than surrounding liver parenchyma. Transient type B: NE was observed transiently in earliest part of early-phase, followed by whole enhancement of the lesion similar to the progression of enhancement in surrounding liver parenchyma. Continuous type: NE was observed continuously during early-phase. Type 1, 2: Liver-specific phase. Type 1: Diffuse enhancement. Type 2: Partial enhancement.

uously during the course of the early-phase (continuous type, 66%). Following the transient NE, 6 lesions showed rapid whole enhancement compared to surrounding liver parenchyma (transient type A, 6/13, 46%), and lesions showed gradual whole enhancement almost the same as surrounding liver parenchyma (transient type B, 7/13, 54%). The grade of enhancement in the lesions with continuous type remained a partial enhancement throughout this phase. Color Doppler revealed AP shunt in 4 of the 6 lesions (66%) with transient type A, but in none of the lesions with transient type B and continuous type. The duration time of NE was 4.0±4.2 s (1-11 s) in transient type A, 8.6±4.2 s (4-13 s) in transient type B, and 20±8.7 s (7-37 s) in continuous type, and the duration of continuous type was significantly longer than those of transient types A and B ($p<0.05$). None of the HCC lesions showed NE pattern.

### Contrast Enhancement at Liver-specific Phase of Hemangioma

Relationship of contrast enhancement between early-phase and liver-specific phase: Twelve lesions showed diffuse enhancement (Type 1, 31%) and 26 lesions showed partial enhancement (Type 2, 69%) at the liver-specific phase **(Figure 2)**. The extent and rapidity of early-phase enhancement in the lesions correlated well with the contrast-enhanced pattern of the liver-specific phase **(Figure 3)**.

Contrast enhancement findings by solo-phase method and changing posture method between hemangioma and HCC: Changes of enhanced area by the solo-phase method are shown in **Figure 4**. The average ratio of the enhanced areas in the liver-specific images after taking early-phase sonograms to those by the solo-phase method was 56% in hemangioma and 7.1% in HCC; none of the lesions showed a decreased enhanced area by this method. When 50% increase was defined as positive result, the change was significantly frequent ($p=0.0002$) in hepatic hemangioma (22/38, 56%) compared to HCC (1/15, 7%), **(Figure 5a)**.

In hemangioma, a positive result by the changing posture method was found in 7 lesions with Type 2 enhancement at the liver-specific phase of the 38 lesions, **(Figure 5b)**. None of HCC lesions showed positive results by this method. However, the frequency of the changes of contrast-enhanced appearances by this method was not statistically significant between hemangioma and HCC ($p=0.0744$).

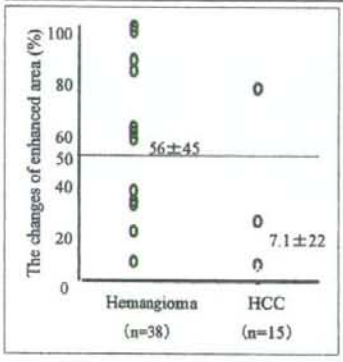


**FIGURE 4** Changes of enhanced area by solo-phase method. Averaged ratios of enhanced area on liver-specific images after taking early-phase sonograms to those by solo-phase method were 56% in hemangioma and 7.1% in HCC.

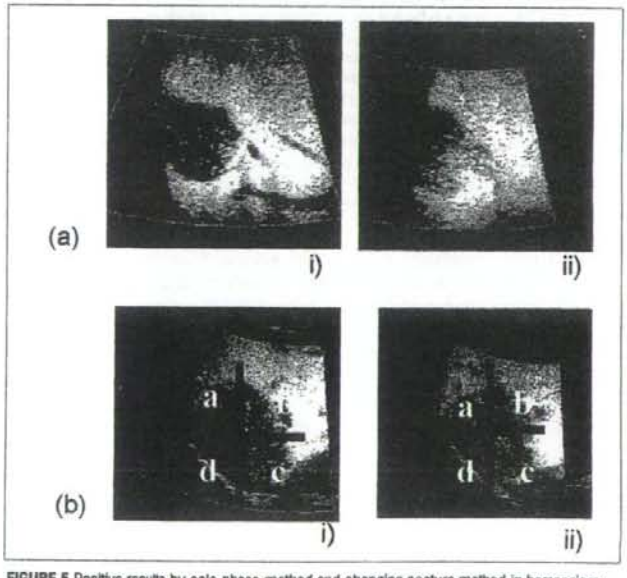


**FIGURE 5** Positive results by solo-phase method and changing posture method in hemangioma. **(a)** Solo-phase method. i) Liver-specific image after taking early-phase sonograms. ii) Liver-specific image without taking early-phase sonograms. Enhanced area increased by 100% with solo-phase method. **(b)** Changing posture method. i) Liver-specific image taken in supine position. ii) Liver-specific image taken by changing posture method. The position with maximum enhancement changed from "b" to "c" in this case.

**Diagnostic Ability of Hemangioma by CEUS with Levovist**

Based on the NE pattern, sensitivity, specificity and accuracy for the diagnosis of hemangioma by CEUS were 100, 100 and 100%, respectively, regardless of the duration of enhancement. However, based on continuous NE, sensitivity, specificity and accuracy were 66, 100, and 66%, respectively. Sensitivity improved by adding the solo-phase method and the changing posture method, from 66 to 79%.

## DISCUSSION

Since cavernous hemangioma is the most common disease among benign liver lesions, improvement of the diagnostic ability is important for management of the disease (8). Because of the non-invasiveness and the convenience of the procedure, US examination as a diagnostic tool of focal liver lesions is viewed with high expectations in clinical practice.

All lesions in the present study showed the NE pattern which is well known as a characteristic pattern of hemangioma in the course of contrast enhancement with Levovist (16-18). However, 34% of the lesions showed this pattern transiently and briefly, and only in the earliest part of the early-phase. As the beginning time of contrast enhancement after the injection of contrast agent depends on each patient, observation of this pattern may not always be certain to allow a diagnosis. These results suggest that the definite diagnosis for hemangioma should not depend solely on NE.

The results of this study suggested that several enhancement patterns of the hemangioma at the early-phase may be related to the in-flow rate of the microbubbles into the lesion, and the existence of AP shunt may be one of the important factors. As the influence of hemangioma with AP shunt is not rare (24,25), the characteristic findings should be noted at CEUS examinations for focal liver lesions. There were 4 hemangiomas accompanied by AP shunt in the present study, and 2 of the 4 hemangiomas showed weak or negative enhancement appearance on liver-specific sonograms. As these lesions showed rapid enhancement in the early-phase with very short duration of NE, such lesions may be confusing in their differentiation from hypervascular HCC by CEUS findings. Additionally, a wedge-shaped enhancement of liver parenchyma adjacent to the lesion was not observed in the early-phase sonograms of the 4 hemangiomas with AP shunt. This finding was somewhat different from the early-phase findings of CECT (24,25). Although the reason is not clear, peripheral liver parenchyma might not be enhanced due to the breakdown of microbubbles via AP shunt by US transmission under high acoustic pressure. The contrast-enhanced appearance of hemangioma with AP shunt should be examined under low acoustic power transmission which provides less microbubble breakdown in further studies. In any event, the extent and rapidity of contrast enhancement of hemangioma by CEUS could be related to the hemodynamic features that may depend on the collective size of the constituent vascular spaces of the lesion (26).

Recently, some next-generation US contrast agents have become available in clinical practice (27). Because of different organ-specific properties, although Levovist and Sonazoid (GE healthcare, Amersham, Oslo, Norway) accumulate in the liver, both Sonovue (Bracco, Milan, Italy) and Definity (Bristol-Myers Squibb, North Billerica, MA) pass through the hepatic sinusoid without accumulation in the liver (28-31). Furthermore, contrary to the usage of Levovist, a low acoustic power level (low MI), which has less microbubbles breakdown, has been frequently applied for these new agents (32,33). This low-MI technique allows continuous scanning, which has the advantage of real-time observation compared to intermittent scanning like the present study (32-35). Therefore, the proper imaging technique and diagnostic results for hemangioma may be different from those using Levovist. The strategy and diagnostic ability for hemangiomas should be investigated for each agent in further studies.

Although positive enhancement in the liver-specific phase is considered as a characteristic finding for benign lesions in the liver (13-15), liver-specific images of hemangiomas was not always homogeneous in the present study, and the findings depended on the early-phase appearance in comparison to HCC. The results of this study suggest that the in-flow of microbubbles in the early-phase may provide the liver-specific findings of hemangioma, and this accounts for the variety of contrast-enhanced findings of hemangioma.

In the present study, 2 novel approaches for the observation of liver-specific phase were applied. According to the result by the solo-phase method, the breakdown of microbubbles caused by the prior observation for the early-phase affected the liver-specific findings of hemangioma. In comparison to the result in HCC, this may be caused by a difference in the in-flow rate of microbubbles into the lesions in the early-phase. The result by the changing posture method suggests that microbubbles of the liver-specific phase in some hemangiomas stay in a mobile state. Accumulation of microbubbles by Kupffer cells is considered one of the causes for the phenomenon (36), however, Tung *et al.* reported that hemangioma lacked Kupffer cell distribution in their pathological examination (19). In addition, the pathological results in a previous study revealed that hemangioma has large sinusoidal vascular spaces that show pooling of contrast material in angiography and CECT (37). Therefore, these stagnant hemodynamics may be related to the liver-specific sonograms of hemangioma, and findings by the changing posture method may reflect this hypothesis. Collectively, it seems that these 2 novel approaches utilizing unique characteristics of Levovist could become optional methods for improvement of the diagnostic ability of hemangioma.

There were some limitations to the present study. First, the improvement of the sensitivity from 66 to 79% for the diagnosis of hemangioma, was assessed by the criteria based on the continuous type of NE alone. Calculated on the basis of any duration of NE pattern, all hemangiomas were able to be diagnosed by the pattern. The development of digital analysis for the quantitative judgment of the existence of NE pattern may help the diagnosis of hemangioma in spite of the short duration of this pattern. Next, regarding the solo-phase method and changing posture method, the results of hemangioma were compared with those of HCC alone. Although these 2 tumors are typical in terms of focal liver lesions, the results should be compared with other kinds of liver tumors. Additionally all HCC patients in the present study had liver cirrhosis which may influence the penetration of US beam. This point may account for the difference of contrast-enhanced findings between hemangioma and HCC. And finally, the results were based on 1 series of US examination in each patient. Confirmation of reproducibility for enhancement findings might be needed in further studies.

In conclusion, cavernous hemangioma in the liver showed various pattern of contrast enhancement in CEUS with Levovist, according to the hemodynamic features of the tumor. With understanding of the backgrounds, CEUS with Levovist may become an essential tool for the diagnosis of hemangioma in the liver.

## REFERENCES


1 **Burns PN, Wilson SR, Simpson DH:** Pulse inversion imaging of liver blood flow: improved method for characterizing focal masses with microbubble contrast. Invest Radiol 2000; 35:58-71.

2 **Maruyama H, Ebara M:** Recent applications of ultrasound: diagnosis and treatment of hepatocellular carcinoma. Int J Clin Oncol 2006; 11:258-267.

3 **Spielmann AL:** Liver imaging with MDCT and high concentration contrast media. Eur J Radiol 2003; 45:S50-S52.

4 **Elsayes KM, Narra VR, Yin Y, et al:** Focal hepatic lesions: diagnostic value of enhancement pattern approach with contrast-enhanced 3D gradient-echo MR imaging. Radiographics 2005; 25:1299-1320.

5 **Nosher JL, Plafker J:** Fine needle aspiration of the liver with ultrasound guidance. Radiology 1980; 136:177-180.

6 **Leen E, Ceccotti P, Kalogeropoulou C, et al:** Prospective multicenter trial evaluating a novel method of characterizing focal liver lesions using contrast-enhanced sonography. AJR Am J Roentgenol 2006; 186:1551-1559.

7 **Kim YK, Kim CS, Chung GH, et al:** Comparison of Gadobenate Dimeglumine-enhanced dynamic MRI and 16-MDCT for the detection of hepatocellular carcinoma. AJR Am J Roentgenol 2006; 186:149-157.

8 **Mergo PJ, Ros PR:** Benign lesions of the liver. Radiol Clin North Am 1998; 36:319-331.

9 **Quinn SF, Benjamin GG:** Hepatic cavernous hemangiomas: simple diagnostic sign with dynamic bolus CT. Radiology 1992; 182:545-548.

10 **Semelka RC, Brown ED, Ascher SM, et al:** Hepatic hemangiomas: a multi-institutional study of appearance on T2-weighted and serial gadolinium-enhanced gradient-echo MR images. Radiology 1994; 192:401-406.

11 **Kim TK, Choi BI, Han JK, et al:** Hepatic tumors: contrast agent-enhancement patterns with pulse-inversion harmonic US. Radiology 2000; 216:411-417.

12 **Isozaki T, Numata K, Kiba T, et al:** Differential diagnosis of hepatic tumors by using contrast enhancement patterns at US. Radiology 2003; 299:798-805.

13 **von Herbay A, Vogt C, Haussinger D:** Late-phase pulse-inversion sonography using the contrast agent Levovist: differentiation between benign and malignant focal lesions of the liver. AJR Am J Roentgenol 2002; 179:1273-1279.

14 **Blomley MJ, Sidhu PS, Cosgrove DO, et al:** Do different types of liver lesions differ in their uptake of the microbubble contrast agent SH U 508A in the late liver phase? Early experience. Radiology 2001; 220:661-667.

15 **Bryant TH, BlomLey MJ, Albrecht T, et al:** Improved characterization of liver lesions with liver-phase uptake of liver-specific microbubbles: prospective multicenter study. Radiology 2004; 232:799-809.

16 **Quaia E, Bertolotto M, Dalla Palma L:** Characterization of liver hemangiomas with pulse inversion harmonic imaging. Eur Radiol 2002; 12:537-544.

17 **Quaia E, Bartolotta TV, Midiri M, et al:** Analysis of different contrast enhancement patterns after microbubble-based contrast agent injection in liver hemangiomas with atypical appearance on baseline scan. Abdom Imaging 2006; 31:59-64.

18 **Bartolotta TV, Midiri M, Quaia E, et al:** Liver haemangiomas undetermined at grey-scale ultrasound: contrast-enhancement patterns with Sonovue and pulse-inversion US. Eur Radiol 2005; 15:685-693.

19 **Tung GA, Cronan JJ:** Percutaneous needle biopsy of hepatic cavernous hemangioma. J Clin Gastroenterol 1993; 16:117-122.

20 **Kim KW, Kim TK, Han JK, et al:** Hepatic hemangiomas with arterioportal shunt: findings at two-phase CT. Radiology 2001; 219:707-711.

21 **Lin ZY, Chang WY, Wang LY, et al:** Clinical utility of pulsed Doppler in the detection of arterioportal shunting in patients with hepatocellular carcinoma. J Ultrasound Med 1992; 11:269-273.

22 **Naganuma H, Ishida H, Konno K, et al:** Hepatic hemangioma with arterioportal shunts. Abdom Imaging 1999; 24:42-46.

23 **Maruyama H, Matsutani S, Okugawa H, et al:** Microbubble disappearance-time is the appropriate timing for liver-specific imaging after injection of Levovist. Ultrasound Med Biol 2006; 32:1809-1815.

24 **Kim KW, Kim AY, Kim, et al:** Hepatic hemangiomas with arterioportal shunt: sonographic appearances with CT and MRI correlation. AJR Am J Roentgenol 2006; 187:W406-W414.

25 **Byun JH, Kim TK, Lee CW, et al:** Arterioportal shunt: prevalence in small hemangiomas versus that in hepatocellular carcinomas 3cm or smaller at two-phase helical CT. Radiology 2004; 232:354-360.

26 **Yamashita Y, Ogata I, Urata J, et al:** Cavernous hemangioma of the liver: pathologic correlation with dynamic CT findings. Radiology 1997; 203:121-125.

27 **Barr R:** Seeking consensus: contrast ultrasound in radiology. Eur J Radiol 2002; 41:207-216

28 **Maruyama H, Matsutani S, Saisho H, et al:** Different behaviors of microbubbles in the liver: time-related quantitative analysis of two ultrasound contrast agents, Levovist® and Definity®. Ultrasound Med Biol 2004; 30:1035-1040.

29 **Forsberg F, Liu JB, Merton DA, et al:** Gray scale second harmonic imaging of acoustic emission signals improves detection of liver tumors in rabbits. J Ultrasound Med 2000; 19:557-563.

30 **Forsberg F, Piccoli CW, Liu JB, et al:** Hepatic tumor detection: MR imaging and conventional US versus pulse-inversion harmonic US of NC100100 during its reticuloendothelial system-specific phase. Radiology 2002; 222:824-829.

31 **Lim AK, Patel N, Eckersley RJ, et al:** Evidence for

spleen-specific uptake of a microbubble contrast agent: a quantitative study in healthy volunteers. Radiology 2004; 231:785-788.

32 **Maruyama H, Matsutani S, Saisho H, et al:** Extra-low acoustic power harmonic images of the liver with perflutren: novel imaging for real-time observation of liver perfusion. J Ultrasound Med 2003; 22:931-938.

33 **Wilson SR, Burns PN:** Liver mass evaluation with ultrasound: the impact of microbubble contrast agents and pulse inversion imaging. Semin Liver Dis 2001; 21:147-159.

34 **Ricci P, Laghi A, Cantisani V, et al:** Contrast-enhanced sonography with SonoVue: enhancement patterns of benign focal liver lesions and correlation with dynamic Gadobenate Dimeglumine-enhanced MRI. AJR Am J Roentgenol 2005; 184:821-827.

35 **Fan ZH, Chen MH, Dai Y, et al:** Evaluation of primary malignancies of the liver using contrast-enhanced sonography: correlation with pathology. AJR Am J Roentgenol 2006; 186:1512-1519.

36 **Iijima H, Moriyasu F, Miyahara T, et al:** Ultrasound contrast agent, Levovist microbubbles are phagocytosed by Kupffer cells-In vitro and in vivo studies. Hepatol Res 2006; 35:235-237.

37 **Freeny PC, Vimont TR, Barnett DC:** Cavernous hemangioma of the liver ultrasonography, arteriography, and computed tomography. Radiology 1979; 132:143-148.

# Down-Regulation of Hedgehog-Interacting Protein through Genetic and Epigenetic Alterations in Human Hepatocellular Carcinoma

Motohisa Tada,[1,3] Fumihiko Kanai,[1,2] Yasuo Tanaka,[1,2] Keisuke Tateishi,[1] Miki Ohta,[1] Yoshinari Asaoka,[1] Motoko Seto,[1] Ryosuke Muroyama,[1] Kenichi Fukai,[3] Fumio Imazeki,[3] Takao Kawabe,[1] Osamu Yokosuka,[3] and Masao Omata[1]

**Abstract** **Purpose:** Hedgehog (Hh) signaling is activated in several cancers. However, the mechanisms of Hh signaling activation in hepatocellular carcinoma (HCC) have not been fully elucidated. We analyzed the involvement of Hh-interacting protein (*HHIP*) gene, a negative regulator of Hh signaling, in HCC.

**Experimental Design:** Glioma-associated oncogene homologue (Gli) reporter assay, 3-(4,5-dimethylthiazol-2-yl)-5-(3-carboxymethoxyphenyl)-2-(4-sulfophenyl)-2H-tetrazolium assay, and quantitative real-time reverse transcription–PCR for the target genes of the Hh signals were performed in *HHIP* stably expressing hepatoma cells. Quantitative real-time PCR for *HHIP* was performed in hepatoma cells and 36 HCC tissues. The methylation status of hepatoma cells and HCC tissues was also analyzed by sodium bisulfite sequencing, demethylation assay, and quantitative real-time methylation-specific PCR. Loss of heterozygosity (LOH) analysis was also performed in HCC tissues.

**Results:** *HHIP* overexpression induced significant reductions of Gli reporter activity, cell viability, and transcription of the target genes of the Hh signals. *HHIP* was hypermethylated and transcriptionally down-regulated in a subset of hepatoma cells. Treatment with a demethylating agent led to the *HHIP* DNA demethylation and restoration of *HHIP* transcription. *HHIP* transcription was also down-regulated in the majority of HCC tissues, and more than half of HCC tissues exhibited *HHIP* hypermethylation. The *HHIP* transcription level in *HHIP*-methylated HCC tissues was significantly lower than in *HHIP*-unmethylated HCC tissues. More than 30% of HCC tissues showed LOH at the *HHIP* locus.

**Conclusions:** The down-regulation of *HHIP* transcription is due to DNA hypermethylation and/or LOH, and Hh signal activation through the inactivation of *HHIP* may be implicated in the pathogenesis of human HCC.

Hepatocellular carcinoma (HCC) is one of the most common cancers in Asia and Africa, and its incidence is increasing worldwide (1). Despite recent advances in early diagnosis and treatment, the prognosis for HCC remains very poor. Most HCC cases arise in the setting of chronic hepatitis virus infection. Alcohol consumption, dietary aflatoxin, and exposure to chemical carcinogens are also implicated in its pathogenesis (1, 2). Although the etiologic factors involved in HCC are well known, the genetic events underlying its carcinogenesis are still unclear.

The Hedgehog (Hh) pathway is indispensable for human development and tissue polarity (3). The binding of secreted Sonic Hh (*SHH*) and Indian Hh to their receptor, patched (*PTCH*), which represses the activity of the transmembrane protein smoothened (*SMO*) in the absence of ligand, leads to alleviation of *PTCH*-mediated suppression of *SMO* (4). Derepression of *SMO* results in the activation of downstream targets through the activation of the transcription factor, glioma-associated oncogene homologue (*GLI*; ref. 4). Two types of aberrant activation of Hh signaling are involved in carcinogenesis: ligand-independent and ligand-dependent activation. The former is due to oncogenic mutation in signal components, such as *SMO* and *PTCH*, and has been reported in sporadic basal cell carcinoma, medulloblastoma, and Gorlin syndrome, which is characterized by numerous basal cell carcinoma, rhabdomyosarcoma, and medulloblastoma (5–9). Ligand-dependent activation with Hh overexpression has been reported in gastric, pancreatic, prostate, and small cell lung cancers (10–14).

Recently, the aberrant activation of Hh signaling in HCC has also been reported (15–17). The authors showed that the overexpression of *SMO* or induced expression of *SHH* was the

**Authors' Affiliations:** Departments of [1]Gastroenterology and [2]Clinical Drug Evaluation, Graduate School of Medicine, University of Tokyo, Tokyo, Japan and [3]Department of Medicine and Clinical Oncology, Graduate School of Medicine, Chiba University, Chiba, Japan

Received 5/15/07; revised 10/13/07; accepted 11/30/07.

The costs of publication of this article were defrayed in part by the payment of page charges. This article must therefore be hereby marked *advertisement* in accordance with 18 U.S.C. Section 1734 solely to indicate this fact.

**Note:** Supplementary data for this article are available at Clinical Cancer Research Online (http://clincancerres.aacrjournals.org/).

**Requests for reprints:** Fumihiko Kanai, Department of Clinical Drug Evaluation, Graduate School of Medicine, University of Tokyo, 7-3-1 Hongo, Bunkyo-ku, Tokyo 113-8655, Japan. Phone: 81-3-3815-5411, ext. 37025; Fax: 81-3-3814-0021; E-mail: kanaif-int@h.u-tokyo.ac.jp.



doi:10.1158/1078-0432.CCR-07-1181

major trigger for Hh signal activation (16, 17). However, the implication of a negative regulator of Hh signaling was not fully investigated. On the other hand, Hh signaling regulates angiogenesis, and Hh-interacting protein (*HHIP*), which functions as a negative regulator of the Hh pathway (18), is down-regulated in endothelial cells during tube formation (19), suggesting that disruption of the *HHIP* gene may induce vascular-rich tumors, such as HCC. This led us to focus on *HHIP*. The *HHIP* gene is expressed in most human fetal and adult tissues (20) and encodes a membrane glycoprotein that binds all three mammalian Hh proteins, i.e., *SHH*, Indian Hh, and Desert Hh, with affinity similar to that of *PTCH* (21). In the current study, we investigated the involvement of *HHIP* in hepatoma cell lines and the methylation status, loss of heterozygosity (LOH), and mRNA expression of *HHIP* gene in 36 HCC cases.

## Materials and Methods

***Cell culture.*** The human hepatoma and hepatoblastoma cell lines HLE, HuH7, HepG2, HuH6, and PLC/PRF/5 were obtained from the Health Science Resources Bank, and Hep3B was obtained from the Cell Resource Center for Biomedical Research. The cell lines were grown in DMEM supplemented with 10% fetal bovine serum, 100 units/mL penicillin, and 100 μg/mL streptomycin.

***Patients.*** Liver tissues were obtained from 36 HCC patients (31 men and 5 women; mean age, 62.3 ± 11.0 y) who underwent surgical resection at Chiba University Hospital. Among these patients, six were positive for hepatitis B surface antigen and 25 were positive for hepatitis C virus antibody, whereas the remaining five patients lacked evidence of either viral infection. Based on the histologic findings, the 36 HCC tumors were classified as follows: 6 well-differentiated, 25 moderately differentiated, and 5 poorly differentiated tumors. More than 50% of the tumors developed in cirrhotic livers (Supplementary Table S1). HCC samples and corresponding nontumor liver tissues obtained by surgical resection were immediately frozen at -80°C. All patients gave informed consent for their participation, and the ethics committee approved these studies.

***Establishment of cells with stable expression of* HHIP.** We purchased the full-length human *HHIP* clone that encodes the open reading frame of *HHIP* from GeneCopoeia and inserted it into the pCMV-Tag4 mammalian expression vector (Stratagene), thereby generating the pCMV-Tag4-*HHIP* vector. After confirming the insertion by sequencing, we transfected the pCMV-Tag4-*HHIP* vector or the empty vector (pCMV-Tag4) using Fugene 6 (Roche) into HuH7 and Hep3B cells, which were confirmed as *HHIP*-null cells by quantitative real-time reverse transcription–PCR (RT-PCR) and Western blotting (Fig. 1; data not shown). To establish cell lines that stably express *HHIP*, we cultured the transfected cells in the presence of 800 μg Geneticin (Wako). Geneticin-resistant colonies appeared within 2 wk, after which the cells were expanded for another 3 wk to produce the original stock cells. Four *HHIP* stable transfectants (H7-HHIP1, H7-HHIP2 and 3B-HHIP1, 3B-HHIP2) and two control transfectants (H7-MOCK and 3B-MOCK) were selected for further study.

***Western blotting.*** Western blotting was done using proteins of total fractions and the primary antibodies for rabbit anti-SHH (1:250; Santa Cruz Biotechnology), rabbit anti-*GLI1* (1:1,000; Cell Signaling Technology), rabbit anti-Hip (R&D Systems), mouse anti–β-actin (*ACTB*; 1:10,000; Sigma-Aldrich), and mouse anti-FLAG M2 (1:1,000; Sigma-Aldrich). The appropriate horseradish peroxidase–conjugated antibodies (1:1,000; Amersham) were used as secondary antibodies. An enhanced chemiluminescence detection system (ECL-plus, Amersham) was used for detection. Experimental procedures were performed as previously described (10).

***Gli reporter assay.*** Hepatoma and hepatoblastoma cells lines, *HHIP* stably transfected cells and the control MOCK cells, were seeded into 12-well plates and grown to ~50% to 70% confluence for 24 h before being transiently transfected with 0.5 μg of 8× 3′Gli-BS-δ51 Luc II, a gift from Dr. Hiroshi Sasaki (Center for Developmental Biology, RIKEN; ref. 22) and 50 ng of pRL-SV40 vector (Toyo Ink) using Fugene 6. This Gli-luciferase reporter construct contains eight copies of the consensus Gli-binding site upstream of a δ-crystallin basal promoter (22, 23). Cells were harvested 48 h after transfection, and luciferase assays were performed with the Picagene Dual Sea Pansy system (Toyo Ink). Firefly and sea pansy luciferase activities were measured as relative light units using a luminometer (Lumat LB 9507, EG&G Berthold). All assays were performed at least in triplicate.

***Cyclopamine treatment.*** All six hepatoma and hepatoblastoma cell lines were seeded into six-well plates and grown in medium containing the pharmacologic Hh inhibitors, cyclopamine (Toronto Research Chemicals) at concentrations of 0 to 10 μmol/L for 96 h. We changed the medium every 2 d.

***3-(4,5-Dimethylthiazol-2-yl)-5-(3-carboxymethoxyphenyl)-2-(4-sulfophenyl)-2H-tetrazolium assay.*** The numbers of viable cells were determined using a CellTiter 96 $AQ_{ueous}$ One Solution Cell Proliferation Assay (Promega) according to the manufacturer's instructions. In brief, cells were plated on six-well tissue culture plates at a density of $3.0 \times 10^4$ per well. Ninety-six hours after seeding, the cells were incubated with 3-(4,5-dimethylthiazol-2-yl)-5-(3-carboxymethoxyphenyl)-2-(4-sulfophenyl)-2H-tetrazolium (MTS) reagent solution for 2 h at 37°C. The absorbance at 490 nm was recorded using an ELISA plate reader. All assays were performed at least in triplicate.

***5-Aza-2′-deoxycitidine treatment.*** For demethylation experiments, all six hepatoma and hepatoblastoma cells were plated at a density of $5.0 \times 10^5$ cells/100-mm dish and cultured for 24 h, followed by 96 h of culturing with 1 μmol/L 5-aza-2′-deoxycitidine (5-aza-CdR; Sigma-Aldrich).

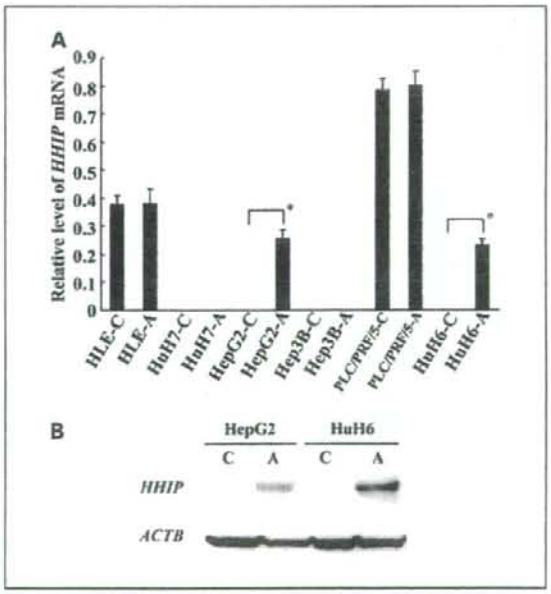


Fig. 1. *A*, relative levels of *HHIP* mRNA expression in hepatoma and hepatoblastoma cell lines. Columns, mean from the results of three independent experiments; bars, SD. *, $P < 0.0001$. *B*, *HHIP* protein expression in HepG2 and HuH6 cells with or without 5-aza-CdR treatment: *C*, control (without 5-aza-CdR treatment); *A*, treated with 5-aza-CdR.

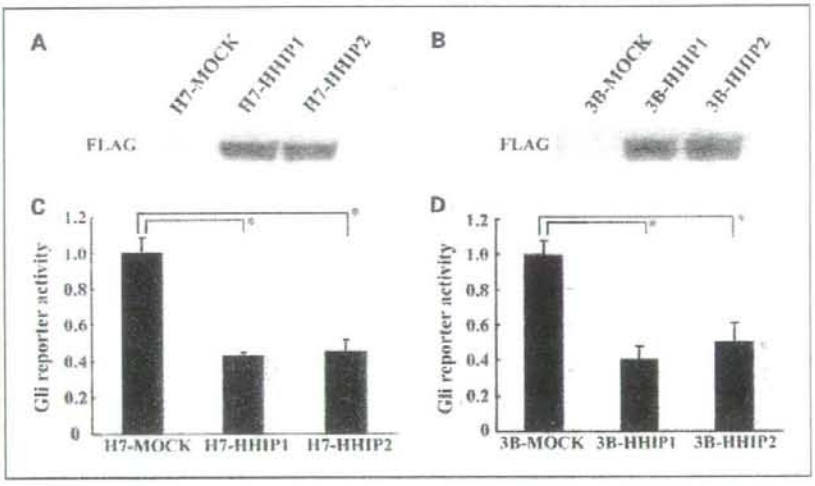


**Fig. 2.** *A* and *B*, establishment of *HHIP* stable transfectant was confirmed by Western blotting. *C* and *D*, Gli reporter activity of *HHIP* stably expressing cells. Ratios to the activity of MOCK cells. Columns, mean from three independent experiments; bars, SD. *, $P < 0.001$.

***Quantitative real-time RT-PCR.*** Three micrograms of total RNA from each sample were subjected to RT reaction using random oligonucleotide primers and Superscript II reverse transcriptase (Invitrogen) according to the manufacturer's instructions. Real-time PCR for *HHIP*, *PTCH*, and *GLI1* genes was performed using the cDNAs of six hepatoma and hepatoblastoma cell lines untreated or treated with 5-aza-CdR, HCC tissues, and corresponding nontumor tissues. Quantitative real-time PCR was also performed for *PTCH*, *GLI1*, B-cell lymphoma protein 2 (*BCL2*), and cyclin D2 (*CCND2*) genes, the downstream target genes of Hh signaling (24–27), using the cDNAs of the *HHIP* stably transfected cells and the control MOCK cells. All assays were performed with the TaqMan Gene Expression Assays Inventoried (*HHIP*, Hs00368450_m1; *PTCH*, Hs00181117_m1; *GLI1*, Hs00171790_m1; *BCL2*, Hs00153350_m1; *CCND2*, Hs00277041_m1; *ACTB*, Hs99999903_m1), TaqMan Universal PCR Master Mix, and ABI Prism 7000 Sequence Detection Systems (Applied Biosystems). The standard curve method was used to calculate target gene expression, which was normalized to that of the *ACTB* gene. Each sample was analyzed in triplicate.

***Sodium bisulfite DNA sequencing.*** Genomic DNA extracted from each of the hepatoma and hepatoblastoma cell lines without 5-aza-CdR treatment was modified by sodium bisulfite using a CpGenome DNA Modification kit (Chemicon International) according to the manufacturer's instructions. The bisulfite-modified DNA was amplified by seminested PCR using the following specific primers: first amplification, forward 5′-AGTAGTYGGGTAGTTTYGGAATT-3′; second amplification, forward 5′-GGTTTAGTATTTTYGAGGTTGGT-3′; and first and second amplifications, reverse 5′-CAACCACAAATATTCACT-TATCC-3′. The PCR products were subcloned into the pCR2.1-TOPO vector using a TA cloning kit (Invitrogen) according to the manufacturer's instructions. To determine the CpG methylation status of the 5′ CpG island of the *HHIP* gene, 10 clones from each cell line were sequenced using the ABI PRISM Dye Deoxy Terminator Cycle Sequencing kit and analyzed in an ABI 310 DNA Sequencer (Applied Biosystems). To confirm DNA demethylation by 5-aza-CdR treatment, the genomic DNA from cells treated with 5-aza-CdR was also subjected to bisulfite sequencing when they exhibited DNA hypermethylation of the *HHIP* gene.

***Quantitative methylation specific real-time PCR.*** Sodium bisulfite–treated genomic DNA samples from the cell lines and liver tissues were analyzed by means of Methylight, a fluorescence-based real-time PCR assay, as described previously (28, 29). Briefly, two sets of primers and probes, designed specifically for bisulfite-converted DNA, were used, a methylated set for *HHIP* and a reference set for *ACTB*, to normalize for input DNA. The specificities of the reactions for methylated DNA were confirmed separately using CpGenome Universal Methylated DNA (Chemicon). The percentage of fully methylated molecules at a specific locus was calculated by dividing the *HHIP/ACTB* ratio of a sample by the *HHIP/ACTB* ratio of Universal Methylated DNA and multiplying by 100. When the percentage of fully methylated reference defined by the above formula above was ≥4%, the *HHIP* gene was deemed to be hypermethylated in the sample (29). The primers and probes for *HHIP* and *ACTB* were as follows: for *HHIP*, forward 5′-GTTGTAGTCGTCGG-TAGAGGAGATT-3′, reverse 5′-ACAAATATTCACTTAT CCGTATAAC-GAA-3′, and probe 5′-FAM-AGTTTAGCGTTGGTTTTG-MGB-3′; for *ACTB*, forward 5′-TGGTGATGGAGGAGGTTTAGTAAGT-3′, reverse 5′-AACCAATAAAACCTACTCCTCCCTTAA-3′, and probe 5′-FAM-ACCAC-CACCC AACACACAATAACA AACACA-TAMRA-3′. Each sample was analyzed in triplicate.

***LOH analysis.*** LOH was investigated using three polymorphic markers of the 4q31.22 region located within 1.5 Mb of the *HHIP* locus (centromeric, D4S1604; very close, D4S2998; telomeric, D4S1586). DNA was amplified by fluorescence PCR (30). The primer sequences used were as follows: for D4S1604, forward 5′-TCGTGCCCAGCCAAGT-3′ and reverse 5′-TTGCTCACAGGATTGCTTCT-3′; for D4S2998, forward 5′-AAGTTCTTGGGCCGCAG-3′ and reverse 5′-TTCTACACCCAGGG-GAACC-3′; for D4S1586, forward 5′-GCATGTACCATTGCCAGG-3′ and reverse 5′-CCCAGAGTGCTGATGTGTG-3′. The PCR products were separated by capillary electrophoresis on an ABI 310 Genetic Analyzer using Genescan and GeneMapper 3.7 software (Applied Biosystems).The LOH index was calculated as follows: the peak height of two alleles in each tumor was divided by the peak height in the corresponding nontumor tissues. LOH was defined by an LOH index of <0.67 or >1.5 (31). Allelic deletion of each gene was judged by positive LOH at any of the three sites.

***Mutation analysis.*** Six hepatoma and hepatoblastoma cell lines were subjected to mutation analysis in the 13 exons of the *HHIP* gene. DNA from these cells was amplified by PCR using the primers designed for the region flanking the intron-exon junction (32). The DNA was sequenced using an ABI PRISM Dye Deoxy Terminator Cycle Sequencing kit and analyzed on an ABI 310 DNA Sequencer (Applied Biosystems).

***Statistical analysis.*** Differences between mean values were evaluated by the unpaired *t* test, and differences in frequencies were evaluated by Fisher's exact test. Results were considered statistically significant at $P < 0.05$.

## Results

*Expression of Hh signaling components and Hh pathway activity in hepatoma and hepatoblastoma cell lines.* To analyze whether Hh signaling is present in hepatoma and hepatoblastoma cell lines, we examined the expression of *SHH* and *GLI1* by Western blotting and *PTCH* expression by quantitative real-time RT-PCR. We also performed Gli reporter assay to investigate Hh pathway activity in these cell lines. The expression of these components and Hh pathway activity were detected in all cell lines to various extents (Supplementary Fig. S1A-C).

**HHIP** *attenuates Hh signaling and induces growth inhibitory effects in hepatoma cell lines.* To investigate whether the transfection of *HHIP* altered the activity of Hh signaling in hepatoma cell lines, we transfected the Gli reporter plasmids into *HHIP* stably transfected cells and the control MOCK cells (Fig. 2A and B) and measured the Gli reporter activity, an indicator of Hh signaling activity, in these cells. The Gli reporter activities in the *HHIP* stably transfected cells were reduced by ~50% to ~60%, compared with that in the MOCK cells ($P < 0.001$; Fig. 2C and D). We also investigated the mRNA expression levels of *PTCH*, *GLI1*, *BCL2*, and *CCND2* genes in *HHIP* stably transfected cells and the control MOCK cells. Compared with the corresponding levels in MOCK cells, the mRNA expression levels of these genes in *HHIP* stably expressing cells were down-regulated by 30% to 40% ($P < 0.01$ or 0.05; Supplementary Fig. S2A and B).

Next, to investigate the effect of *HHIP* on the growth of hepatoma cell lines, the MTS assay was performed on *HHIP* stably transfected cells. After 96 hours of culture, the viabilities of the *HHIP* stably transfected cells were ~40% lower than those of the MOCK cells ($P < 0.001$; Fig. 3A and B).

**HHIP** *transcription is down-regulated through hypermethylation of 5′ CpG islands in hepatoma and hepatoblastoma cell lines.* Quantitative real-time RT-PCR analysis revealed that the *HHIP* transcript was undetectable in HuH7, Hep3B, HepG2, and HuH6 cells without 5-aza-CdR treatment, whereas it was abundant in HLE and PLC/PLF/5 cells (Fig. 1A). Treatment with 5-aza-CdR significantly restored *HHIP* mRNA expression in HepG2 and HuH6 cells ($P < 0.0001$; Fig. 1A). The restoration of *HHIP* protein was also confirmed by Western blotting in HepG2 and HuH6 cells (Fig. 1B). *HHIP* transcription in HuH7 and Hep3B cells remained undetectable after 5-aza-CdR treatment. The HLE and PLC/PRF/5 cells, with high initial expression of *HHIP*, exhibited no additional induction of *HHIP* transcription after 5-aza-CdR treatment (Fig. 1A).

The methylation status of the 46 CpG dinucleotides encompassing the promoter region was examined (Fig. 4A). The 5′ CpG island of *HHIP* was densely methylated in each HepG2 clone and was partially methylated in HuH6 cells, both of which showed up-regulation of *HHIP* transcription after 5-aza-CdR treatment, whereas in the HLE, HuH7, Hep3B, and PLC/PRF/5, few of the CpG dinucleotides were methylated. After treatment with 5-aza-CdR, the DNAs of the HepG2 and HuH6 cells were demethylated (Fig. 4B).

*Hh signaling was down-regulated after 5-aza-CdR treatment in HepG2 and HuH6 cells.* In HepG2 and HuH6 cells, in which *HHIP* expression increases after demethylation, the mRNA expressions of *GLI1* and *PTCH* were statistically significantly reduced, by ~25% to 30%, after 5-aza-CdR treatment compared with those of 5-aza-CdR–untreated cells ($P < 0.01$; Supplementary Fig. S3A and B).

*Cell lines without expression of* **HHIP** *tend to be more sensitive to cyclopamine treatment.* To explore the relationship of *HHIP* expression and the sensitivities to cyclopamine in hepatoma and hepatoblastoma cell lines, we investigated the viabilities of cyclopamine-treated cells by MTS assay. MTS assay revealed that the viabilities of HuH7, Hep3B, HepG2, and HuH6 cells, which have no *HHIP* expression, were significantly reduced by treatment with >1 μmol/L of cyclopamine ($P < 0.0001$), whereas treatment with 10 μmol/L of cyclopamine only led to a significant reduction in cell viabilities in HLE and PLC/PRF/5 cells, in which the *HHIP* gene was expressed (Supplementary Fig. S4).

*Lack of* **HHIP** *mutations in hepatoma and hepatoblastoma cells.* Six hepatoma and hepatoblastoma cell lines were screened for evidence of mutations in the 13 exons of the *HHIP* gene. Direct sequencing revealed a complete lack of *HHIP* mutations in these cell lines.

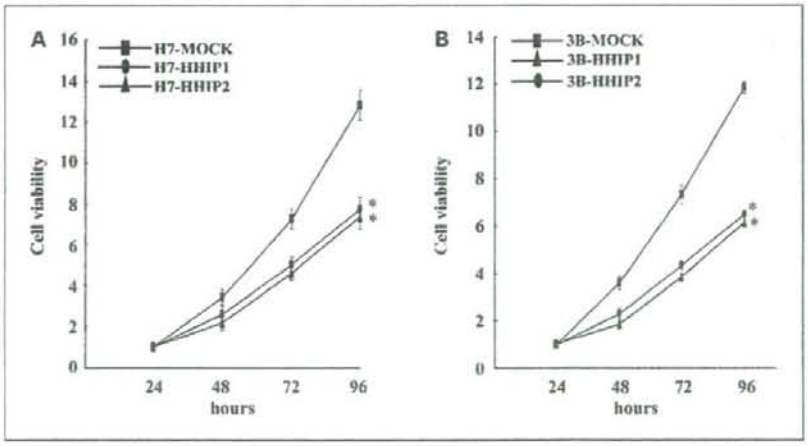


Fig. 3. Viabilities of *HHIP* stably expressing cells. *A*, HuH7 cells. *B*, Hep3B cells. Points, mean from three independent experiments; bars, SD. *, $P < 0.001$.

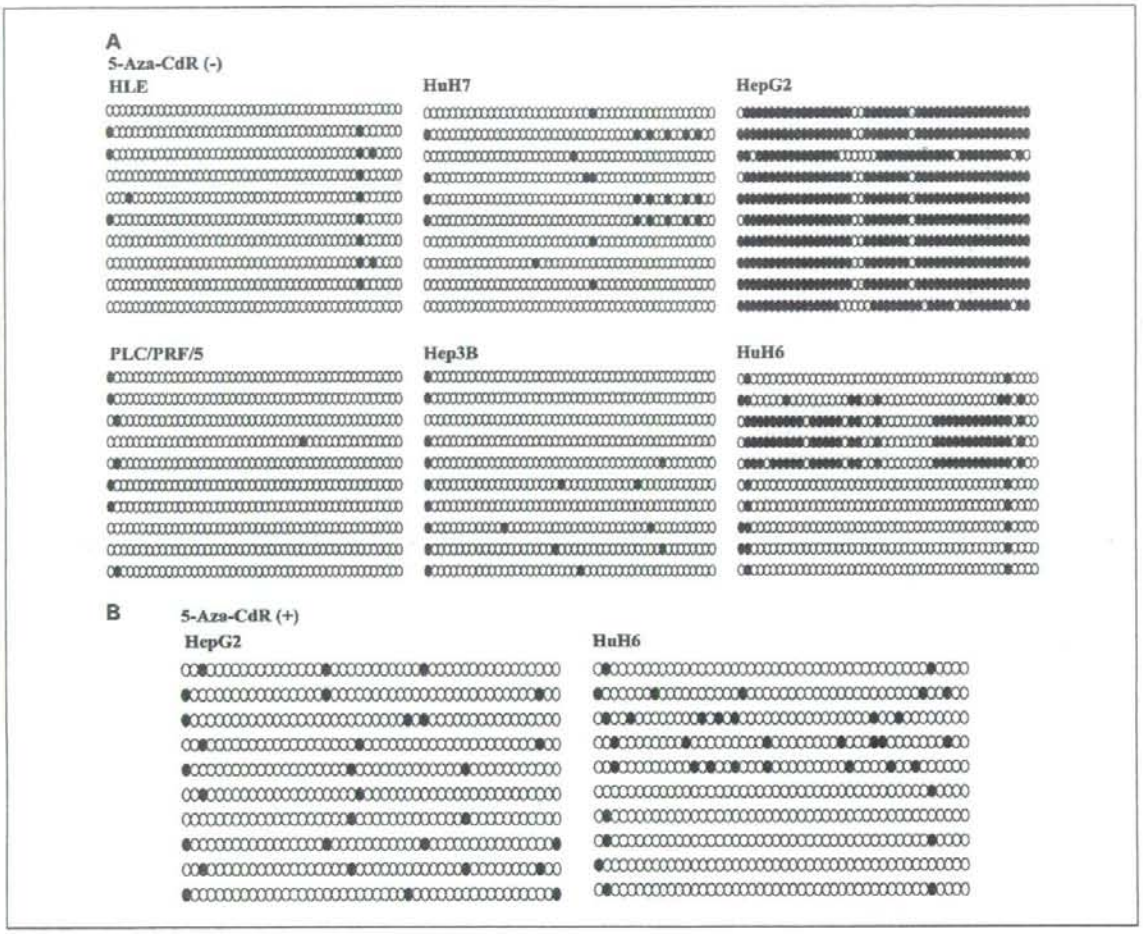


Fig. 4. Methylation status of 46 CpG dinucleotides in the promoter region of the *HHIP* gene. *A*, without 5-aza-CdR treatment; *B*, with 5-aza-CdR treatment. Each circle indicates a CpG site in the primary DNA sequence, and each line of circles represents the analysis of a single cloned allele. Closed circles, methylated CpG dinucleotides; open circles, unmethylated CpG dinucleotides.

**HHIP *DNA is hypermethylated in HCC tissues.*** The occurrence of *HHIP* gene hypermethylation in 36 HCC cases was analyzed using quantitative real-time methylation-specific PCR, Methylight. In the present study, the *HHIP* gene was defined as being hypermethylated in tissues when the percentage of fully methylated reference value was ≥4. The 5′CpG island of the *HHIP* gene was shown as being hypermethylated in 21 of 36 tumors (53.6%), whereas, in the corresponding nontumor liver tissues, *HHIP* hypermethylation was not detected (Table 1). In addition, the percentage of fully methylated reference values of the *HHIP* gene were significantly higher in the tumors than in the corresponding nontumor liver tissues ($5.62 \pm 6.39$ versus $0.19 \pm 0.28$, $P < 0.0001$; Fig. 5A). In the 36 HCC patients, no significant correlation was found between *HHIP* hypermethylation and clinicopathologic characteristics, including sex, age, etiology, state of surrounding liver, differentiation, and size (Supplementary Table S2).

***LOH at* HHIP *gene locus in HCC tissues.*** DNA samples from 36 HCC tissues were examined for LOH at the *HHIP* gene locus using fluorescent PCR. At the D4S1604 locus, 26 of 36 cases (72.2%) were heterozygous and 7 of 26 (26.9%) showed LOH. At the D4S2998 locus, 32 of 36 cases (88.9%) were heterozygous and 10 of 32 (31.3%) showed LOH. The heterozygosity of the D4S1586 locus was 23 of 36 (63.9%), and 5 of 23 (21.7%) exhibited LOH (Supplementary Table S3). In total, heterozygosity was achieved in 32 of 36 cases (88.9%), and LOH at the *HHIP* locus was detected in 10 of 32 cases (31.3%). Of the 10 cases with LOH at the *HHIP* locus, seven also showed *HHIP* DNA hypermethylation. No significant correlation was found between *HHIP* LOH and clinicopathologic characteristics of the 36 HCC patients (Supplementary Table S4).

**HHIP *mRNA expression is down-regulated in HCC tissues.*** The relative level of *HHIP* mRNA was determined by

quantitative real-time RT-PCR as the ratio to the level of *ACTB* mRNA. In 31 of 36 HCC tissues (86.1%), the level of *HHIP* transcription was lower than in the corresponding nontumor tissues (Table 1), and *HHIP* mRNA expression in the HCC tissues was significantly lower than in the corresponding nontumor tissues (3.47 ± 5.84 versus 27.61 ± 34.82, $P < 0.0001$; Fig. 5B). Of the 31 HCC tissues with down-regulated *HHIP* transcription, 7 (22.6%) exhibited both *HHIP* DNA hypermethylation and LOH at the *HHIP* locus and 24 (77.4%) showed either *HHIP* DNA hypermethylation or LOH (Supplementary Table S5). There was no case with *HHIP* DNA hypermethylation or LOH at the *HHIP* locus that had a higher level of *HHIP* transcription in the tumor than in the corresponding nontumor tissues. The expression of *HHIP* mRNA in the tumor was significantly lower in cases with *HHIP* DNA hypermethylation or LOH at the *HHIP* locus than in cases showing DNA unmethylation or retention of heterozygosity (0.25 ± 0.47 in hypermethylation cases and 7.97 ± 6.91 in unmethylation cases, $P < 0.0001$; 0.73 ± 1.19 in LOH cases and 5.27 ± 6.73 in retention of heterozygosity cases, $P < 0.05$; Supplementary Fig. S5A and B). There was no statistically significant correlation between *HHIP* transcription and the clinicopathologic characteristics of the 36 HCC patients (Supplementary Fig. S6).

***GLI1* and *PTCH* mRNA expression in HCC cases.** To assess Hh signaling activation in HCC, we investigated *GLI1* and *PTCH* mRNA expression by quantitative real-time RT-PCR in 36 HCC tissues and corresponding nontumor tissues. We found that *GLI1* mRNA transcription was significantly higher in tumors than in corresponding nontumor tissues (1.78 ± 3.77 versus 0.30 ± 0.65, $P < 0.05$; Supplementary Fig. S7A) whereas *PTCH* mRNA expression tended to be higher in tumors than in corresponding nontumor tissues, although the difference was not statistically significant (31.11 ± 51.27 versus 12.73 ± 27.79, $P = 0.063$; Supplementary Fig. S7B). In addition, mRNA expression of *GLI1* and *PTCH* in tumors tended to be higher in the cases with *HHIP* DNA hypermethylation than in those showing *HHIP* DNA unmethylation, although the difference was not statistically significant (2.69 ± 4.74 versus 0.50 ± 0.65, $P = 0.086$, for *GLI1*, and 43.81 ± 62.15 versus 13.32 ± 21.72, $P = 0.078$, for *PTCH*; Supplementary Fig. S8A and B). These results suggested that Hh signaling was activated and that *HHIP* methylation might be implicated in Hh signal activation in HCC.

## Discussion

HCC is one of the most frequent human cancers worldwide and has a very poor prognosis (1), despite advances in early diagnosis and therapy. Several studies have indicated that the accumulation of genetic changes occurs in a stepwise manner during the development and progression of HCC, as well as other human cancers. However, the molecular mechanisms underlying the pathogenesis of HCC have not been fully elucidated.

It is well known that aberrant activation of Hh signaling is involved in carcinogenesis. Oncogenic mutation of the Hh pathway has been detected in Gorlin syndrome, sporadic basal cell carcinoma, and medulloblastoma (5–9). On the other hand, overexpression of the ligand in the Hh pathway has been shown to cause pathway activation in gastric, pancreatic, prostate, and small cell lung carcinoma (10–14). It has been reported that the Hh pathway is also activated in HCC (15–17). In our study, as well, Hh signaling components were expressed in hepatoma and hepatoblastoma cell lines to various degrees. Hh signaling plays a major role in multiple aspects of embryonic development, including that of the liver (33), although mature hepatocytes lack Hh signaling activity (11). Therefore, it is possible that the remaining Hh signal-responsive progenitor cells function as cancer stem cells in the liver, leading to the genesis of HCC. The overexpression of *SMO* or *SHH*, positive regulators of the Hh pathway, has been shown to be the major trigger for Hh signal activation (16, 17). However, proto-oncogenes are rarely altered in HCC, suggesting that inactivation of tumor suppressor genes is critical for hepatocarcinogenesis (34). Therefore, we focused on the *HHIP* gene, a

**Table 1.** DNA methylation, mRNA expression and LOH status of *HHIP* gene in HCC cases

| Case no. | DNA methylation | | LOH | mRNA expression (T/NT) |
|---|---|---|---|---|
| | T | NT | | |
| 1 | +* | - | +† | 0.006 |
| 2 | + | - | + | 0.001 |
| 3 | + | - | - | 0.055 |
| 4 | - | - | - | 1.125 |
| 5 | + | - | + | 0.127 |
| 6 | - | - | - | 0.303 |
| 7 | + | - | - | 0.028 |
| 8 | - | - | - | 0.295 |
| 9 | + | - | - | 0.051 |
| 10 | + | - | NI | 0.008 |
| 11 | + | - | - | 0.044 |
| 12 | + | - | + | 0.016 |
| 13 | - | - | + | 0.033 |
| 14 | + | - | - | 0.002 |
| 15 | - | - | - | 1.079 |
| 16 | - | - | - | 1.093 |
| 17 | + | - | - | 0.004 |
| 18 | - | - | - | 2.396 |
| 19 | + | - | - | 0.007 |
| 20 | - | - | - | 0.050 |
| 21 | - | - | - | 0.209 |
| 22 | + | - | + | 0.001 |
| 23 | + | - | - | 0.004 |
| 24 | + | - | + | 0.0024 |
| 25 | + | - | NI | 0.009 |
| 26 | - | - | - | 0.707 |
| 27 | + | - | - | 0.012 |
| 28 | + | - | + | 0.012 |
| 29 | + | - | - | 0.007 |
| 30 | + | - | - | 0.002 |
| 31 | - | - | - | 3.889 |
| 32 | + | - | - | 0.009 |
| 33 | - | - | + | 0.104 |
| 34 | - | - | NI | 0.011 |
| 35 | - | - | NI | 0.095 |
| 36 | - | - | + | 0.084 |

Abbreviations: T, tumor; NT, nontumor; +, positive; -, negative; NI, not informative.

*When the value of PMR was ≥4 in the sample, *HHIP* DNA was defined as hypermethylated, otherwise *HHIP* DNA was defined as unmethylated.

†When LOH was detected at any of three markers used in this analysis, LOH status of *HHIP* gene was defined as positive.

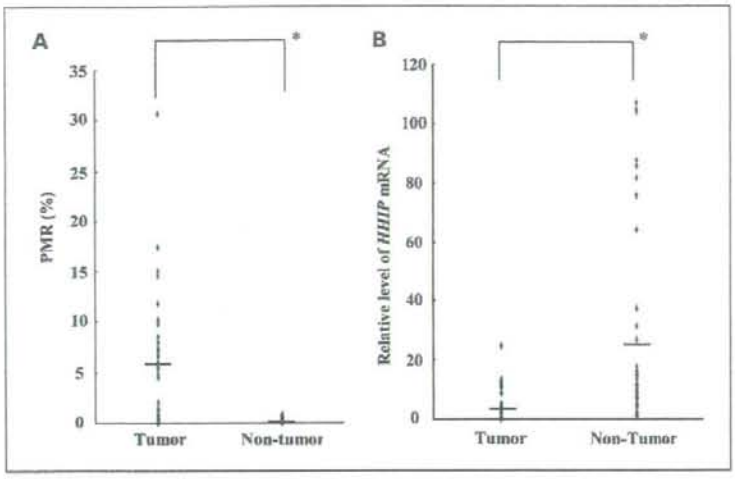


Fig. 5. *A*, methylation status of *HHIP* in 36 HCC tissues and corresponding nontumor liver tissues, as detected by quantitative real-time methylation-specific PCR (Methylight). PMR, percentage of fully methylated reference. Bar in the middle, mean percentage of fully methylated reference; points, mean from triplicate assays. *, $P < 0.0001$. *B*, *HHIP* mRNA expression in 36 HCC tissues and corresponding nontumor tissues. Bar in the middle, mean level of *HHIP* mRNA expression; points, mean from triplicate assays. *, $P < 0.0001$.

negative regulator of Hh signaling (18), and investigated the involvement of *HHIP* in HCC.

In the current study, transfection of the full-length *HHIP* expression vector into two *HHIP*-null cell lines (HuH7 and Hep3B) led to significant reductions in cell viabilities, Gli-reporter activities, and the *PTCH* and *GLI1* transcripts, which are indicators of Hh signal activation. Transfection of full-length mouse *HHIP* into mouse testicular epithelial cells (TM3) attenuated their responses to *SHH*, which shows that *HHIP* antagonizes Hh signaling when expressed in responding cells (19). Concordant with this, *HHIP* also attenuated Hh signal activation in hepatoma cells, with consequent growth inhibition. Treatment with cyclopamine, a plant steroidal alkaloid that inhibits the cellular response to the Hh signal (35), also led to reductions in cell viabilities and Hh signal activation in hepatoma cell lines (15–17).Thus, the effect of the overexpression of *HHIP* is similar to that of cyclopamine on hepatoma cell lines.

In our study, cyclopamine was also observed to cause reduction in cell viabilities. Moreover, interestingly, sensitivities to cyclopamine were higher in *HHIP*-null cell lines than in *HHIP*-expressing cell lines. Cyclopamine antagonizes *SMO* (35), but not *HHIP*, so the cause of these differences in the sensitivities to cyclopamine in hepatoma cell lines remains to be elucidated. *HHIP* expression, however, might be useful for the prediction of cyclopamine responsiveness.

To elucidate the involvement of the downstream genes of Hh signaling in *HHIP*-overexpressed hepatoma cells, we investigated the mRNA expression of *BCL2* and *CCND2* genes, downstream target genes in the Hh pathway (26, 27). *HHIP* overexpression resulted in the down-regulation of *BCL2* and *CCND2* transcription, suggesting that the *HHIP*-mediated reduction of hepatoma cell viabilities may be due to an increase in apoptosis or cell cycle arrest.

In our study, there was no correlation between intrinsic *HHIP* expression and Hh signal activation, which was surrogated by *GLI1* protein expression, Gli reporter assay, and *PTCH* mRNA expression. This may be due to other mechanisms for the regulation of *GLI1* and *PTCH* expression.

*HHIP* expression is decreased in several human tumors of the lung, stomach, colorectal tract, and liver compared with the corresponding normal tissues (15, 19), although *HHIP* is expressed in most fetal and adult tissues (20). In the present study, *HHIP* mRNA expression was down-regulated in a subset of hepatoma and hepatoblastoma cell lines, and its expression in the majority of HCC tissues was much lower than in the corresponding nontumor liver tissues, in concordance with previous reports (15, 19). To elucidate the mechanisms of the down-regulation of *HHIP* expression, methylation and LOH analyses were performed.

Promoter hypermethylation has recently been identified as a hallmark of human cancer (36). Aberrant CpG island hypermethylation is clearly associated with transcriptional silencing of gene expression and plays an important role in the mechanism by which tumor suppressor genes are inactivated in cancer (37, 38). The inactivation through DNA hypermethylation of several tumor suppressor genes, such as *E-cadherin*, $p16^{INK4a}$, *SOCS*, *14-3-3σ*, and *GSTP1*, has also been reported in HCC (39–43).

In the present study, we showed that *HHIP* mRNA transcription is down-regulated through *HHIP* DNA hypermethylation in a subset of hepatoma and hepatoblastoma cell lines. Quantitative methylation-specific PCR, Methylight, revealed that *HHIP* DNA was also hypermethylated in >50% of the HCC tissues, although methylation was not detected in the corresponding nontumor liver tissues, and the level of *HHIP* transcription was significantly lower in hypermethylated HCC tissues than that in unmethylated HCC tissues, suggesting that down-regulation of *HHIP* transcription can be attributed to aberrant hypermethylation of the *HHIP* gene in HCC. Aberrant methylation of the *HHIP* gene has also been reported in gastrointestinal and pancreatic cancers (32, 44).

Moreover, the *GLI1* and *PTCH* transcription levels tended to be higher in *HHIP*-methylated HCC than in *HHIP*-unmethylated HCC, meaning that the down-regulation of *HHIP* transcription through *HHIP* hypermethylation might lead to Hh signal activation in HCC. The reason why the difference in *GLI1* and *PTCH* mRNA expression levels between methylated

HCCs and unmethylated HCCs was not statistically significant could be that there were other regulatory mechanisms for Hh signaling in HCC (16, 17).

*HHIP* transcription was also down-regulated in HuH7 and Hep3B cells while the *HHIP* DNA was not methylated and 5-aza-CdR treatment did not lead to restoration of *HHIP* transcription in these cells. However, genome-wide LOH analysis of hepatoma cell lines using a high-density single-nucleotide polymorphism array and a data analysis tool, Copy Number Analyzer for Affymetrix GeneChip Mapping 100K arrays (45), revealed LOH of the *HHIP* locus in HuH7 and Hep3B cells.[4] Moreover, because the *HHIP* gene is located at 4q31.22 and chromosome 4q is frequently deleted in HCC (46, 47), we investigated the LOH status of the *HHIP* locus. LOH analysis revealed that 31.3% (10 of 32) of the HCC tissues exhibited LOH at the *HHIP* gene locus, and the *HHIP* transcription level was significantly lower in HCC tissues showing LOH of *HHIP* than in HCC tissues showing retention of heterozygosity of *HHIP*. These results suggest that LOH is one of the mechanisms by which *HHIP* mRNA is down-regulated in HCC.

For the 31 HCC tissues in which *HHIP* mRNA expression was down-regulated compared with the corresponding nontumor liver tissues, 7 tissues exhibited both *HHIP* DNA hypermethylation and LOH at the *HHIP* locus, 14 tissues showed only *HHIP* hypermethylation, and 3 tissues showed only LOH. To elucidate additional mechanisms for the down-regulation of the *HHIP* gene, mutational analysis was performed. Although this analysis was not performed with HCC tissues, we detected no mutation in any of the 13 exons of the *HHIP* gene in all the hepatoma and hepatoblastoma cell lines. Similarly, a recent study found no mutation in the *HHIP* gene in pancreatic cancer cell lines and primary pancreatic cancers (32).

Although somatic inactivation of tumor suppressor genes is usually achieved by the loss of the chromosomal region that spans the first allele and by promoter hypermethylation or intragenic mutations in the second allele, some tumor suppressor genes may require only one genetic or epigenetic alteration if inactivation of one allele leads to haploinsufficiency of the protein (48). Therefore, *HHIP* may represent this type of tumor suppressor gene.

Seven HCC tissues in which *HHIP* mRNA expression was down-regulated, compared with corresponding nontumor liver tissues, showed neither *HHIP* DNA hypermethylation nor LOH. Although the cause of the *HHIP* down-regulation in these cases is unknown, the possible involvement of some novel somatic mutation and/or additional regulatory mechanisms, such as regulation by microRNA, might be worthy of consideration.

In previous studies, the overexpression of *SMO* or *SHH* was shown to be the major trigger for Hh signal activation in HCC (16, 17). However, the mechanisms of these overexpressions in HCC have not yet been determined. In addition, although the authors detected a novel mutation of *SMO* in a single HCC case (16), this type of mutation is rare and is less common than hypermethylation and/or LOH of *HHIP*.

In conclusion, we have shown that *HHIP* overexpression led to a reduction in hepatoma cell viabilities and that the restoration of *HHIP* transcription by demethylating agent in *HHIP*-hypermethylated cells attenuated Hh signaling. Moreover, we have shown that *HHIP* transcription is down-regulated and that down-regulation of *HHIP* transcription can be attributed to aberrant DNA hypermethylation or LOH of *HHIP* in a subset of hepatoma cell lines and in the majority of HCC tissues. Ectopic expression of *SHH* leads to ectopic *HHIP* expression, indicating that *HHIP* is a transcriptional target of Hh signaling (21). However, in the present study, we have shown that DNA hypermethylation and LOH are involved in the Hh signal-independent regulation of *HHIP* transcription in HCC. Hh signal activation through the inactivation of *HHIP* may have implication for the pathogenesis of human HCC.

## Acknowledgments

We thank Mitsuko Tsubouchi for technical assistance and Dr. H. Sasaki (RIKEN Center for Developmental Biology) for supplying the key materials.

[4] M. Tada, F. Kanai, Y. Tanaka, M. Sanada, et al., unpublished data.

## References

1. Harris CC. Hepatocellular carcinogenesis: recent advances and speculations. Cancer Cell 1990;2:146–8.
2. Okuda K. Hepatocellular carcinoma: recent progress. Hepatology 1992;15:948–63.
3. Pasca di Magliano M, Hebrok M. Hedgehog signalling in cancer formation and maintenance. Nat Rev Cancer 2003;3:903–11.
4. Evangelista M, Tian H, de Sauvage FJ. The hedgehog signaling pathway in cancer. Clin Cancer Res 2006;12:5924–8.
5. Johnson RL, Rothman AL, Xie J, et al. Human homolog of patched, a candidate gene for the basal cell nevus syndrome. Science 1996;272:1668–71.
6. Hahn H, Wicking C, Zaphiropoulous PG, et al. Mutations of the human homolog of *Drosophila* patched in the nevoid basal cell carcinoma syndrome. Cell 1996;85:841–51.
7. Xie J, Murone M, Luoh SM, et al. Activating Smoothened mutations in sporadic basal-cell carcinoma. Nature 1998;391:90–2.
8. Reifenberger J, Wolter M, Weber RG, et al. Missense mutations in SMOH in sporadic basal cell carcinomas of the skin and primitive neuroectodermal tumors of the central nervous system. Cancer Res 1998;58:1798–803.
9. Raffel C, Jenkins RB, Frederick L, et al. Sporadic medulloblastomas contain PTCH mutations. Cancer Res 1997;57:842–5.
10. Ohta M, Tateishi K, Kanai F, et al. p53-Independent negative regulation of p21/cyclin-dependent kinase-interacting protein 1 by the sonic hedgehog-glioma-associated oncogene 1 pathway in gastric carcinoma cells. Cancer Res 2005;65:10822–9.
11. Berman DM, Karhadkar SS, Maitra A, et al. Widespread requirement for Hedgehog ligand stimulation in growth of digestive tract tumours. Nature 2003;425:846–51.
12. Thayer SP, di Magliano MP, Heiser PW, et al. Hedgehog is an early and late mediator of pancreatic cancer tumorigenesis. Nature 2003;425:851–6.
13. Karhadkar SS, Bova GS, Abdallah N, et al. Hedgehog signalling in prostate regeneration, neoplasia and metastasis. Nature 2004;431:707–12.
14. Watkins DN, Berman DM, Burkholder SG, Wang B, Beachy PA, Baylin SB. Hedgehog signalling within airway epithelial progenitors and in small-cell lung cancer. Nature 2003;422:313–7.
15. Patil MA, Zhang J, Ho C, Cheung ST, Fan ST, Chen X. Hedgehog signaling in human hepatocellular carcinoma. Cancer Biol Ther 2006;5:111–7.
16. Sicklick JK, Li YX, Jayaraman A, et al. Dysregulation of the Hedgehog pathway in human hepatocarcinogenesis. Carcinogenesis 2006;27:748–57.
17. Huang S, He J, Zhang X, et al. Activation of the hedgehog pathway in human hepatocellular carcinomas. Carcinogenesis 2006;27:1334–40.
18. Chuang PT, Kawcak T, McMahon AP. Feedback control of mammalian Hedgehog signaling by the Hedgehog-binding protein, Hip1, modulates Fgf signaling during branching morphogenesis of the lung. Genes Dev 2003;17:342–7.
19. Olsen CL, Hsu PP, Glienke J, Rubanyi GM, Brooks AR. Hedgehog-interacting protein is highly expressed in endothelial cells but down-regulated during angiogenesis and in several human tumors. BMC Cancer 2004;4:43.
20. Bak M, Hansen C, Friis Henriksen K, Tommerup N. The human hedgehog-interacting protein gene: structure and chromosome mapping to 4q31.21→q31.3. Cytogenet Cell Genet 2001;92:300–3.
21. Chuang PT, McMahon AP. Vertebrate Hedgehog

signalling modulated by induction of a Hedgehog-binding protein. Nature 1999;397:617–21.
22. Sasaki H, Hui C, Nakafuku M, Kondoh H. A binding site for Gli proteins is essential for HNF-3β floor plate enhancer activity in transgenics and can respond to Shh *in vitro*. Development 1997;124:1313–22.
23. Kamachi Y, Kondoh H. Overlapping positive and negative regulatory elements determine lens-specific activity of the δ1-crystallin enhancer. Mol Cell Biol 1993;13:5206–15.
24. Marigo V, Tabin CJ. Regulation of patched by sonic hedgehog in the developing neural tube. Proc Natl Acad Sci U S A 1996;93:9346–51.
25. Lee J, Platt KA, Censullo P, Ruiz i Altaba A. Gli1 is a target of Sonic hedgehog that induces ventral neural tube development. Development 1997;124:2537–52.
26. Bigelow RL, Chari NS, Unden AB, et al. Transcriptional regulation of bcl-2 mediated by the sonic hedgehog signaling pathway through gli-1. J Biol Chem 2004;279:1197–205.
27. Yoon JW, Kita Y, Frank DJ, et al. Gene expression profiling leads to identification of GLI1-binding elements in target genes and a role for multiple downstream pathways in GLI1-induced cell transformation. J Biol Chem 2002;277:5548–55.
28. Eads CA, Danenberg KD, Kawakami K, et al. MethyLight: a high-throughput assay to measure DNA methylation. Nucleic Acids Res 2000;28:E32.
29. Eads CA, Lord RV, Kurumboor SK, et al. Fields of aberrant CpG island hypermethylation in Barrett's esophagus and associated adenocarcinoma. Cancer Res 2000;60:5021–6.
30. Luo L, Shen GQ, Stiffler KA, Wang QK, Pretlow TG, Pretlow TP. Loss of heterozygosity in human aberrant crypt foci (ACF), a putative precursor of colon cancer. Carcinogenesis 2006;27:1153–9.
31. Lin JK, Chang SC, Yang YC, Li AF. Loss of heterozygosity and DNA aneuploidy in colorectal adenocarcinoma. Ann Surg Oncol 2003;10:1086–94.
32. Martin ST, Sato N, Dhara S, et al. Aberrant methylation of the Human Hedgehog interacting protein (HHIP) gene in pancreatic neoplasms. Cancer Biol Ther 2005;4:728–33.
33. Deutsch G, Jung J, Zheng M, Lora J, Zaret KS. A bipotential precursor population for pancreas and liver within the embryonic endoderm. Development 2001;128:871–81.
34. Tada M, Omata M, Ohto M. Analysis of ras gene mutations in human hepatic malignant tumors by polymerase chain reaction and direct sequencing. Cancer Res 1990;50:1121–4.
35. Taipale J, Chen JK, Cooper MK, et al. Effects of oncogenic mutations in Smoothened and Patched can be reversed by cyclopamine. Nature 2000;406:1005–9.
36. Herman JG. Hypermethylation of tumor suppressor genes in cancer. Semin Cancer Biol 1999;9:359–67.
37. Baylin SB, Herman JG, Graff JR, Vertino PM, Issa JP. Alterations in DNA methylation: a fundamental aspect of neoplasia. Adv Cancer Res 1998;72:141–96.
38. Jones PA, Laird PW. Cancer epigenetics comes of age. Nat Genet 1999;21:163–7.
39. Kanai Y, Ushijima S, Hui AM, et al. The E-cadherin gene is silenced by CpG methylation in human hepatocellular carcinomas. Int J Cancer 1997;71:355–9.
40. Liew CT, Li HM, Lo KW, et al. High frequency of p16INK4A gene alterations in hepatocellular carcinoma. Oncogene 1999;18:789–95.
41. Yoshikawa H, Matsubara K, Qian GS, et al. SOCS-1, a negative regulator of the JAK/STAT pathway, is silenced by methylation in human hepatocellular carcinoma and shows growth-suppression activity. Nat Genet 2001;28:29–35.
42. Iwata N, Yamamoto H, Sasaki S, et al. Frequent hypermethylation of CpG islands and loss of expression of the 14-3-3σ gene in human hepatocellular carcinoma. Oncogene 2000;19:5298–302.
43. Zhong S, Tang MW, Yeo W, Liu C, Lo YM, Johnson PJ. Silencing of GSTP1 gene by CpG island DNA hypermethylation in HBV-associated hepatocellular carcinomas. Clin Cancer Res 2002;8:1087–92.
44. Taniguchi H, Yamamoto H, Akutsu N, et al. Transcriptional silencing of hedgehog-interacting protein by CpG hypermethylation and chromatic structure in human gastrointestinal cancer. J Pathol 2007;213:131–9.
45. Nannya Y, Sanada M, Nakazaki K, et al. A robust algorithm for copy number detection using high-density oligonucleotide single nucleotide polymorphism genotyping arrays. Cancer Res 2005;65:6071–9.
46. Zimonjic DB, Keck CL, Thorgeirsson SS, Popescu NC. Novel recurrent genetic imbalances in human hepatocellular carcinoma cell lines identified by comparative genomic hybridization. Hepatology 1999;29:1208–14.
47. Guan XY, Fang Y, Sham JS, et al. Recurrent chromosome alterations in hepatocellular carcinoma detected by comparative genomic hybridization. Genes Chromosomes Cancer 2000;29:110–6.
48. Payne SR, Kemp CJ. Tumor suppressor genetics. Carcinogenesis 2005;26:2031–45.

*Hepatology Research* 2008; 38: 535–542 doi: 10.1111/j.1872-034X.2008.00323.x

***Review Article***

# Current antiviral therapies for chronic hepatitis B

Mari Inada and Osamu Yokosuka

*Department of Medicine and Clinical Oncology, Postgraduate School of Medicine, Chiba University, Chiba, Japan*

Among current treatment options for chronic hepatitis B, nucleoside/nucleotide analog therapy has better tolerability and most patients respond to the therapy, while interferon (IFN) therapy has rather severe side-effects and a lower response rate. However, nucleoside/nucleotide analog therapies have problems of the emergence of drug resistance and poor sustainability of response after discontinuation. After the first nucleoside/nucleotide analog lamivudine, adefovir and entecavir are now utilized in many countries. Adefovir has efficacy for lamivudine resistant patients and current data suggests that adding adefovir to ongoing lamivudine is better than switching to adefovir in terms of viral suppression and the occurrence of resistance. Entecavir can be the first choice for naïve patients, although cross-resistance has been known for lamivudine resistant patients and mutational screening should take place before using entecavir with such patients. Many other new nucleoside/nucleotide analogs are being developed such as telbivudine, clevudine and tenofovir; the details of each drug will be disclosed in near future.

**Key words:** Lamivudine, adefovir, entecavir, telvibudine, clevudine, tenefovir

## INTRODUCTION

THE TREATMENT OF chronic hepatitis B remains a worldwide agenda. Two billion people are estimated to be infected with the virus and about 400 million of these have chronic hepatitis B.[1] Chronic hepatitis B is a common cause of mortality, responsible for 0.5–1.2 million deaths annually from liver cirrhosis and hepatocellular carcinoma (HCC).[2–4] As hepatitis B virus (HBV) itself is not a cytotoxic virus, chronic hepatitis B is thought to be caused by an immunological response of the host against the viral proteins.[5–7] Therefore the suppression of HBV replication is important for the treatment of chronic hepatitis B from the point of preventing the formation of viral proteins. Circulating HBV particles enter into the hepatocytes and after the formation of complete double-stranded DNA, covalently closed circular DNA (cccDNA) is made from the relaxed circular DNA.[8] The production of pregenome RNA from the cccDNA is important for active HBV replication.[9,10] HBV has a reverse-transcription process from the pregenome RNA to HBV-DNA in its replication cycle,[11] and this process would be blocked by reverse transcriptase inhibitors. Current major treatment options are immunomodulatory and viral suppressant drugs, interferon (IFN)/pegylated (PEG) IFN or nucleoside/nucleotide analogs. These two types of therapies have different effects, each with their own merits and demerits. In this review, treatment with nucleoside/nucleotide analogs, especially drugs recently approved in Japan – adefovir and entecavir – are discussed.

*Correspondence: Professor Osamu Yokosuka, Department of Medicine and Clinical Oncology, Postgraduate School of Medicine, Chiba University, 1-8-1 Inohana, Chuou Ward, Chiba City, Chiba 260-8670, Japan. Email: yokosukao@faculty.chiba-u.jp*
*Received 1 October 2007; revision 5 December 2007; accepted 9 December 2007.*

## AIM OF TREATMENT

THE MAJOR AIM of therapy for HBV is to prevent the progression of the disease to cirrhosis, end stage liver disease or HCC.[12–15] The ideal end point of the treatment is HBsAg loss and the formation of anti-HBsAb, however, this rarely happens.[16] Practically it is reasonable to infer improvement in disease outcome by suppressing HBV replication, with an accompanying improvement in serum alanine aminotransferase (ALT) and hepatic necroinflammation[17] and, in HBeAg positive patients, followed by HBeAg loss or HBe seroconversion.

## TREATMENT OPTIONS

TWO MAJOR GROUPS of antiviral therapies are currently utilized for the treatment of HBV, IFN-α or PEG IFN-α, and nucleoside/nucleotide analogs. Treatment with IFN/PEG IFN-α is of finite duration and the response is often durable after treatment, however this treatment has side-effects and a relatively small number of patients respond, although higher viral clearance can be expected than with nucleoside/nucleotide analogs.[18] Recent studies have revealed that the response to IFN is different among HBV genotypes. We can expect a better sustained response to standard IFN-α in HBeAg positive genotype B patients than genotype C patients, and in genotype A patients than genotype D patients.[19–21] With PEG IFN-α, the HBe Ag seroconversion rate was 47%, 44%, 28% and 25% in genotype A, genotype B, genotype C and genotype D patients, respectively.[22] The distribution of HBV genotypes differs in each area of the world.[23–24] In Japan, 85% of chronic hepatitis B patients are genotype C, which is known to have higher risk of HCC at an earlier age than genotype B,[25–27] and the effect of IFN is limited, so in such areas other therapies may be required.[28–29]

In contrast, nucleoside/nucleotide analogs are well tolerated and most patients respond to therapy, but treatment is hampered by the selection of drug resistant mutants, leading to a loss of efficacy and frequent relapse after discontinuation. Usually, cccDNA is resistant to the treatment and remains in the hepatocytes even after long-term treatment, so by the discontinuation of the drugs the HBV replication restarts from the remaining HBV-RNA produced from the cccDNA and relapse occurs promptly.[30] A high level of HBV-RNA may predict the early emergence of a resistant strain.[31] So far the efficacy of nucleoside/nucleotide analogs has been reported to be almost the same among genotypes, but each genotype showed a difference in the occurrence rate of resistant mutants to lamivudine.[32] In addition, the durability of the therapy may be less in genotype C than in genotype B patients.[33]

Among nucleoside/nucleotide analogs, lamivudine was the first drug to be utilized, and because of its potency, safety profile and relatively low cost, it has been and still is widely applied globally as the first choice of therapy.[34,35] However, the relatively high occurrence of resistance is recognized; 70% within 4 years.[36–40] It has been reported that there are differences in the occurrence of resistant strains among HBV genotypes. Studies from Japan showed that genotype C, genotype Bj and genotype Ba had resistance to lamivudine in 50%, 28% and 13% of patients, respectively, within 2 years, and genotype A, which is now increasing in number in Japan, has an even higher rate of resistance.[41,42] Genotypes will be one of the important factors in choosing the therapy as we accumulate more data.

Another important problem for lamivudine is how and when the treatment should be discontinued. Combinations with lamivudine, with interferon, or HBV vaccination have been tried but their effects are still unknown.[43,44] There are reports that reduction of the levels of HBV core related antigen may suggest the timing of the discontinuation.[45,46]

For patients who have already developed resistance to it, substituting or adding other antiviral agents is necessary. Now, many other new nucleoside/nucleotide analogs have been developed, and several studies are ongoing to decide which of the available nucleoside/nucleotide analogs should be the first line therapy, although it remains difficult to pinpoint, for there is insufficient data to compare each of them; more data is needed on drug efficacy and genotypes. The data currently available will be shown below.

## ADEFOVIR

ADEFOVIR DIPIVOXIL IS an orally bioavailable prodrug of adefovir, a phosphonate acyclic nucleotide analog of adenosine monophosphate.[47] Adefovir acts by selectively inhibiting the reverse transcriptase-DNA polymerase of HBV by direct binding in competition with the endogenous substrate deoxyadenosine triphosphate (dATP).[48] Adefovir lacks a-3'hydroxyl group and, after incorporation into the nascent viral DNA, results in the premature termination of viral DNA synthesis. Unlike other nucleoside analogs such as lamivudine, adefovir is monophosphorylated and is not dependent on initial phosphorylation by viral nucleoside kinases to exert its antiviral effect.

### Adefovir monotherapy

With adefovir 1-year monotherapy, the decline of viral load was 3.6–5.7 $\log_{10}$ copies/mL in HBeAg positive patients and 3.9 in HBeAg negative patients. HBV-DNA negativity of less than the lower limit of detection (LLD), which was 200 copies/mL by polymerase chain reaction (PCR), after 1 year of therapy was 28–39%. ALT normalization was achieved in 48–81% of HBeAg positive patients and 72% of HBeAg negative patients. HBeAg loss was reported in 13–24%, HBe seroconversion in 8–18% and HBsAg loss in 0% of patients.[49–52] There is no apparent difference in the efficacy of adefovir